

PM/97-25  
 UFR-HEP/98-09  
 August 1998

# Radiative corrections to $e^+e^- \rightarrow H^+H^-$ : THDM versus MSSM .

A. Arhrib<sup>a,b¶</sup>, G. Moultaka<sup>c||</sup>

*a: Département de Mathématiques, Faculté des Sciences et Techniques,  
 B.P 416 Tanger Morocco*

*b: UFR-Physique des Hautes Energies, Faculté des Sciences  
 PO Box 1014, Rabat-Morocco*

*c: Laboratoire de Physique Mathématique et Théorique, CNRS-UMR 5825  
 Université Montpellier II, F-34095 Montpellier Cedex 5, France*

## Abstract

One loop radiative corrections to  $e^+e^- \rightarrow H^+H^-$  are considered at future linear collider energies, in the general type II Two Higgs Doublet Model (THDM) and in the Minimal Supersymmetric Standard Model (MSSM). To make easy the comparison between THDM and MSSM, we have introduced a quasi-SUSY parameterization which preserves all the tree-level Higgs mass-sum-rules of the MSSM, and involves just 3 free parameters in the Higgs sector (instead of 7 in the general THDM) and comprises the MSSM as a particular case. The model-independent soft photon contribution is isolated and shown to be substantial. Important effects come also from the contribution of the model dependent  $h^0H^+H^-$  and  $H^0H^+H^-$  vertices to the final state. In the MSSM, the contribution of the Higgs sector is moderate (a few percent) while in the THDM and both for small and large  $\tan\beta$  important effects ( $\sim +30\%$ ) can be found.

---

¶E-mail:arhrib@fstt.ac.ma

||E-mail:moultaka@lpm.univ-montp2.fr

# 1 Introduction

Supersymmetry is one of the most promising scenarios in terms of which one can approach new physics at the present and next generation of colliders (LEPII, upgraded CDF, LHC, LC2000,...). In this context, the awaited discovery of a neutral Higgs particle, if successful, will need to be complemented by the discovery and study of the full-fledged Higgs sector as well as the purely supersymmetric sector, in order to test unambiguously the Minimal Supersymmetric Standard Model (MSSM) [1] or possibly its non-minimal extensions [2].

Such a task will presumably be rather intricate as any realistic supersymmetric model predicts a plethora of particles and associated couplings. It should also comprise a full test of the various mass-sum-rules and relations among the couplings endemic to supersymmetry [3], these being, in some cases, sensibly modified by radiative corrections [4, 5].

These large modifications can be crucial in the experimental search strategy. Perhaps the most illustrative example is the loosening of the MSSM tree-level mass bound for the lightest CP-even Higgs from

$$m_{h^0} \leq M_Z \quad \text{to} \quad m_{h^0} \leq M_Z + g^2 \frac{m_t^4}{M_Z^2} \ln\left(\frac{m_t^2}{m_t^2}\right)$$

by loop effects [4, 5], which raises the mass bound to  $\sim 130$  GeV below which the lightest Higgs should be discovered or else the MSSM ruled out.

Sizeable modifications of tree-level predictions are likely to occur not only in the Higgs mass-sum-rules[6] but also in Higgs self-couplings, and more moderately in mass relations and couplings in the chargino, neutralino, squark, slepton and gluino sectors. Some of these have been already looked at [7] in a model dependent context, however ultimately a systematic exploration of all regions of susy parameters leading to potentially large deviations that can affect tree level relations as well as production and decay rates of new particles, would become mandatory in order to achieve full tests of susy. Indeed there is a *priori* no guarantee that moderate corrections to a given observable will ensure moderate corrections to all other observables related to the same given sector.

The subject of the present paper is the one-loop electroweak corrections to the charged Higgs pair production in  $e^+e^-$  collisions. This will turn out to be precisely an example where important effects are present in the production cross-section, even though corrections to the  $H^\pm$  mass sum rule are known to be modest [8]. ( Loop corrections to  $H^\pm$  decays are also important to study [9] but will not be considered in this paper).

Generally speaking, a charged scalar particle coupled to fermions proportionally to their masses is a by-product of an extended Higgs sector with scalar fields in non-singlet representations of the weak symmetry. As such its experimental discovery would thus be immediate qualitative evidence in favor of a structure beyond the standard model, in contrast with the neutral Higgs which would necessitate a more quantitative investigation. Present experimental direct search for charged Higgses set lower bound on its mass. At LEP-II search, ALEPH and OPAL Collaborations set a lower bound of 52 GeV and DELPHI Collaboration sets a lower bound of 54.4 GeV [10]. At the Tevatron, CDF collaboration has searched for charged Higgs decay of the top quark excluding a charged Higgs

mass lower than  $\sim 147$  GeV in the large  $\tan\beta$  limit [11]. However, using the Tevatron quark data in the lepton plus  $\tau$  a lower mass limit of 100 GeV for  $\tan\beta \geq 40$  has been reported [12]. For a recent discussion of the LEP and Tevatron limits and a reappraisal see [13]

Indirect limits, valid only in the non supersymmetric case, have been inferred from  $b \rightarrow s\gamma$  and read [14]:

$$M_{H^\pm} > 244 \text{GeV} + \frac{63}{\tan\beta^{1.3}} \text{GeV}$$

see also [15].

Although supersymmetry can generically invalidate the previous indirect limit, some studies suggest that useful bounds can still be inferred in some model-dependent cases (assuming grand unified minimal supergravity and a negative Higgs mass parameter  $\mu$  [16]). At hadronic machines, future direct production of charged Higgses can proceed either via pair production through gluon-gluon fusion [17] or the less favoured  $q\bar{q}$  annihilation Drell-Yan process[18], or via single production in association with quarks[19] or a  $W$  boson[20]. On the other hand, the charged Higgs can be efficiently searched for only when its top-bottom decay mode is kinematically forbidden [otherwise one would have to look at bosonic decay modes ex.  $H^\pm \rightarrow h^0 W^\pm$ ,  $H^\pm \rightarrow A^0 W^\pm$ , etc... [18], see also [13]].

The future  $e^+e^-$  machines will presumably offer a cleaner environment and in that sense a higher mass reach, especially if the 1–2TeV options are available. There the charged Higgs can be produced either in pairs through  $\gamma, Z$  exchange[21], or in single rare production in association with a  $W$  boson [22]. The former channel has at tree-level the particularity of depending only on standard model parameters, it is thus important to understand the trend of loop effects which contain the model dependence.

The one-loop electroweak corrections to  $e^+e^- \rightarrow H^+H^-$  have been previously considered at NLC energies, restricting mainly to top-bottom, squarks and sleptons contributions [23]. Prominent effects were found from either sectors and for large regions of the parameter space. Also no generic drastic cancellation between fermion and sfermion contributions was found so that the net total effect can easily range from  $-30\%$  to  $+30\%$  depending on the various parameters. In the present paper we complete the study by including the effects of the remaining sectors. A summary of the results was already given in [24]. Let us also mention here that charged Higgs pair production through laser back-scattered  $\gamma\gamma$  collisions has been studied in the literature at the tree as well as the one-loop levels [25] reaching similar conclusions as to the importance of the quantum corrections.

In view of the potentially large corrections the first issue here will be mainly (but not exclusively), to pin down all possible large effects from other sectors than the ones considered in [23]. For this we present the full set of one-loop corrections in a general type II two-Higgs-doublet model (THDM-II), that is the complete Higgs sector contributions (self-energies, vertices and boxes), the infrared part including initial and final soft photon radiation,  $\gamma\gamma$ ,  $\gamma Z$  and  $WW$  boxes, as well as the (standard) initial state vertex and fermion and gauge boson self-energies contributions. THDM-II, besides being interesting in its own

right, is a relevant framework in terms of which to assess the sensitivity to supersymmetric effects.

The second issue will be to parameterize the comparison between THDM-II and the more constrained MSSM cases. Indeed it will turn out that apart from large model independent contributions in the infrared sector, important effects are found in diagrams involving triple Higgs couplings, however only in the non-supersymmetric case. In order to assess the sensitivity to such effects it will be appropriate to define an effective parameterization where all the ( tree-level ) MSSM Higgs mass-sum-rules remain valid while some of the tree-level triple Higgs couplings deviate from their MSSM form. This parameterization which we will dub “quasi-supersymmetric” necessitates just one extra free parameter ( instead of five) in the Higgs sector, as compared to the MSSM and actually offers a general setting to quantify the tests of the self-couplings in the Higgs sector.

Finally we also evaluate the full set of box diagrams involving virtual charginos, neutralinos, selectron and sneutrino states, in order to pursue the comparison between THDM-II and MSSM.

The rest of the paper is organized as follows. In section II we review the main features of the Higgs potential in THDM-II as well as in the MSSM. We then define and discuss the “quasi-supersymmetric” parameterization which interpolates between the two models and recall the form of the various Higgs couplings. In section III the tree-level production cross-section is presented and some notations and conventions defined. Section IV is devoted to the general form of the radiative corrections and to a description of the various contributions. In section V we describe the renormalization scheme which is most suited in our case to a comparison between the supersymmetric and non-supersymmetric cases, and discuss as well the Infrared sector. Section VI is devoted to the numerical analysis, and section VII to the conclusion. Finally, presentation of complementary analytic expressions and technical details of the calculation is relegated to the appendices.

## 2 The relevant Lagrangian and the “quasi-susy” parameterization.

In this section we focus on the structure of the charged Higgs couplings to the other Higgs fields and recall as well its couplings to the gauge bosons and matter fermions, excluding the supersymmetric sector. We will refrain from presenting extensively the various features of the Higgs potential, as this has been repeatedly achieved in the literature <sup>1</sup> The aim here is rather to identify the tree-level couplings which can carry information about the presence of supersymmetry, distinguishing them from those which have the same form whether susy is operative or not. We then encompass these features in a suitable general parameterization.

---

<sup>1</sup>we follow throughout this section the notations of [26] to which we refer the reader for relevant details

## 2.1 The two-Higgs doublet potential

Assuming two complex  $SU(2)_{weak}$  doublet scalar fields  $\Phi_1$  and  $\Phi_2$  defined as

$$\Phi_1 = \begin{pmatrix} \phi_1^+ = \varphi_1 + i\varphi_2 \\ \phi_1^0 = \varphi_3 + i\varphi_4 \end{pmatrix} \quad \Phi_2 = \begin{pmatrix} \phi_2^+ = \varphi_5 + i\varphi_6 \\ \phi_2^0 = \varphi_7 + i\varphi_8 \end{pmatrix}$$

the most general (dimension 4)  $SU(2)_{weak} \times U(1)_Y$  gauge invariant and (CP-invariant) scalar potential is given by (see, however, the Errata in ref [26]):

$$\begin{aligned} V(\Phi_1, \Phi_2) = & \lambda_1(\Phi_1^+ \Phi_1 - v_1^2)^2 + \lambda_2(\Phi_2^+ \Phi_2 - v_2^2)^2 + \lambda_3((\Phi_1^+ \Phi_1 - v_1^2) + (\Phi_2^+ \Phi_2 - v_2^2))^2 \\ & + \lambda_4((\Phi_1^+ \Phi_1)(\Phi_2^+ \Phi_2) - (\Phi_1^+ \Phi_2)(\Phi_2^+ \Phi_1)) + \lambda_5(Re(\Phi_1^+ \Phi_2) - v_1 v_2)^2 + \\ & \lambda_6 Im(\Phi_1^+ \Phi_2)^2 + \lambda_7 \end{aligned} \quad (1)$$

where  $\Phi_1$  and  $\Phi_2$  have weak hypercharge  $Y=1$  and the  $\lambda_i$ 's are real-valued. We will also assume the arbitrary additive constant  $\lambda_7$  to be vanishing. This would of course be the case if exact supersymmetry is imposed, and should any way be required for a vanishing cosmological constant (at least as a tree-level approximation). No other assumptions on the  $\lambda_i$ 's are made except that they sit in the regions that allow the required pattern of spontaneous electroweak symmetry breaking down to  $U(1)_{ew}$  [27].

The minimum of the potential is then obtained for

$$\langle \Phi_1 \rangle = \begin{pmatrix} v_1 \\ 0 \end{pmatrix} \quad \langle \Phi_2 \rangle = \begin{pmatrix} v_2 \\ 0 \end{pmatrix}$$

After the Higgs mechanism has taken place, the W and Z gauge boson acquire masses given by  $m_W^2 = \frac{1}{2}g^2 v^2$  and  $m_Z^2 = \frac{1}{2}(g^2 + g'^2)v^2$ , where  $g$  and  $g'$  are the  $SU(2)_{weak}$  and  $U(1)_Y$  gauge couplings and  $v^2 = v_1^2 + v_2^2$ . The combination  $v_1^2 + v_2^2$  is thus fixed by the electroweak scale through  $v_1^2 + v_2^2 = (2\sqrt{2}G_F)^{-1}$  and we are left with 7 free parameters in eq.(1), namely the  $\lambda_i$ 's and  $v_2/v_1$ .

On the other hand, three of the eight degrees of freedom of the two Higgs doublets correspond to the 3 goldstone bosons, the remaining five become the physical Higgs bosons  $H^0, h^0$  (CP-even),  $A^0$  (CP-odd) and  $H^\pm$ . Their masses are obtained as usual from the shift  $\Phi_i \rightarrow \Phi_i + \langle \Phi_i \rangle$  and read

$$m_{A^0}^2 = \lambda_6 v^2 ; \quad m_{H^\pm}^2 = \lambda_4 v^2 \quad \text{and} \quad m_{H^0, h^0}^2 = \frac{1}{2}[A + C \pm \sqrt{(A - C)^2 + 4B^2}] \quad (2)$$

where

$$A = 4v_1^2(\lambda_1 + \lambda_3) + v_2^2\lambda_5 , \quad B = v_1 v_2(4\lambda_3 + \lambda_5) \quad \text{and} \quad C = 4v_2^2(\lambda_2 + \lambda_3) + v_1^2\lambda_5 \quad (3)$$

The angle  $\beta$  given by  $\tan \beta = v_2/v_1$  defines the mixing leading to the physical  $H^\pm$  and  $A^0$  states, while the mixing angle  $\alpha$  associated to  $H^0, h^0$  physical states is given by [See ref [26] for further details.]

$$\sin 2\alpha = \frac{2B}{\sqrt{(A-C)^2 + 4B^2}}, \quad \cos 2\alpha = \frac{A-C}{\sqrt{(A-C)^2 + 4B^2}} \quad (4)$$

It will be more suitable for the forthcoming discussion to trade the five parameters  $\lambda_{1,2,4,5,6}$  for the 4 Higgs masses and the mixing angle  $\alpha$ . From now on we will take the physical Higgs masses,  $m_{H^0}, m_{h^0}, m_{A^0}, m_{H^\pm}$ , the mixing angles  $\alpha, \beta$  and the coupling  $\lambda_3$  as the 7 free parameters.

It is then straightforward algebra to invert equations (2) through (4), and get the  $\lambda_i$ 's in terms of this new set of parameters.

$$\lambda_4 = \frac{g^2}{2m_W^2} m_{H^\pm}^2 \quad \lambda_6 = \frac{g^2}{2m_W^2} m_A^2 \quad (5)$$

$$\lambda_5 = \frac{g^2}{2m_W^2} \frac{\sin 2\alpha}{\sin 2\beta} (m_H^2 - m_h^2) - 4\lambda_3 \quad (6)$$

$$\lambda_1 = \frac{g^2}{16 \cos^2 \beta m_W^2} [m_H^2 + m_h^2 + (m_H^2 - m_h^2) \frac{\cos(2\alpha + \beta)}{\cos \beta}] + \lambda_3 (-1 + \tan^2 \beta) \quad (7)$$

$$\lambda_2 = \frac{g^2}{16 \sin^2 \beta m_W^2} [m_H^2 + m_h^2 + (m_h^2 - m_H^2) \frac{\sin(2\alpha + \beta)}{\sin \beta}] + \lambda_3 (-1 + \cot^2 \beta) \quad (8)$$

Using the above expressions, and after having expressed eq.(1) in terms of the Goldstone and physical Higgs fields, one can cast all couplings of the scalar potential in terms of the new set of free parameters.

Here we restrict ourselves to all 3-point vertices (see eqs. (A.1–A.5) of appendix A) involving a charged Higgs field, since these are the only ones that enter one-loop calculations in  $e^+e^- \rightarrow H^+H^-$  (4-point vertices involving  $H^\pm$  have vanishing contributions). Injecting eq.(5–8) in eqs. (A.1–A.5) we get the various couplings in terms of the new set of free parameters,

$$\begin{aligned} g_{H^0 H^+ H^-} = & -i \frac{g}{m_W} [\cos(\beta - \alpha) (m_{H^\pm}^2 - \frac{m_H^2}{2}) + \frac{\sin(\alpha + \beta)}{\sin 2\beta} \{4\lambda_3 v^2 + \frac{1}{2} (m_H^2 + m_h^2) \\ & - \frac{1}{2 \sin 2\beta} (\sin 2\alpha + 2 \sin(\alpha - \beta) \cos(\alpha + \beta)) (m_H^2 - m_h^2)\}] \end{aligned} \quad (9)$$

$$\begin{aligned} g_{h^0 H^+ H^-} = & -i \frac{g}{m_W} [\sin(\beta - \alpha) (m_{H^\pm}^2 - \frac{m_h^2}{2}) + \frac{\cos(\alpha + \beta)}{\sin 2\beta} \{4\lambda_3 v^2 + \frac{1}{2} (m_H^2 + m_h^2) \\ & - \frac{1}{2 \sin 2\beta} (\sin 2\alpha + 2 \sin(\alpha + \beta) \cos(\alpha - \beta)) (m_H^2 - m_h^2)\}] \end{aligned} \quad (10)$$

$$g_{H^0 H^\pm G^\mp} = \frac{-i g \sin(\beta - \alpha) (m_{H^\pm}^2 - m_H^2)}{2m_W} \quad (11)$$

$$g_{h^0 H^\pm G^\mp} = \frac{i g \cos(\beta - \alpha) (m_{H^\pm}^2 - m_h^2)}{2m_W} \quad (12)$$

$$g_{A^0 H^\pm G^\mp} = \mp \frac{v}{\sqrt{2}} (\lambda_6 - \lambda_4) = \mp \frac{m_{H^\pm}^2 - m_A^2}{v\sqrt{2}} \quad (13)$$

It is noteworthy that  $\lambda_3$  enters only  $g_{H^0 H^+ H^-}$  and  $g_{h^0 H^+ H^-}$  while  $g_{H^0 H^\pm G^\mp}$ ,  $g_{h^0 H^\pm G^\mp}$  and  $g_{A^0 H^\pm G^\mp}$  have automatically their MSSM form, however, without assuming the MSSM mass-sum-rules. As we will see in the next subsection, a direct consequence when MSSM mass-sum-rules are assumed, will be that  $\lambda_3$  measures the “amount” of “hard” susy breaking, and that among the five couplings, only  $g_{H^0 H^+ H^-}$  and  $g_{h^0 H^+ H^-}$  are sensitive to such a breaking. We should also stress that no constraint has been imposed thus far, in the derivation of the preceding expressions. In particular no sign assignments for the trigonometric functions of  $\alpha$  or  $\beta$  where made ( apart of course from the definition  $\tan \beta \equiv v_2/v_1 > 0$  )

## 2.2 The “quasi-susy” parameterization

We proceed hereafter to the definition of a partly constrained parameterization which interpolates between the free THDM case, and the constrained MSSM, in the following sense:

- a) It preserves *all* tree-level mass-sum-rules of the MSSM, including the relation between  $\tan 2\alpha$  and  $\tan 2\beta$ <sup>2</sup>;
- b) It needs just 3 free parameters (instead of 7) and comprises the susy case as a special case with 2 free parameters;

Actually such a parameterization would be phenomenologically very natural in case where more than one Higgs particle is discovered, with masses consistent with the MSSM sum-rules. Indeed, taking these sum-rules as granted, one can devise a strategy for further precision tests of the supersymmetric self-Higgs couplings, where a reduced number of free parameters is involved and particularly sensitive sectors are identified .

Let us first recall the situation when softly broken supersymmetry is imposed in eq.(1). As shown in [26] one has the following relations among the  $\lambda_i$ ’s:

$$\begin{aligned} \lambda_1 &= \lambda_2 \quad , \quad \lambda_3 = \frac{1}{8}(g^2 + g'^2) - \lambda_1 \quad , \quad \lambda_4 = 2\lambda_1 - \frac{1}{2}g'^2 \\ \lambda_5 &= -\frac{1}{2}(g^2 + g'^2) + 2\lambda_1 \quad , \quad \lambda_6 = -\frac{1}{2}(g^2 + g'^2) + 2\lambda_1 \end{aligned} \quad (14)$$

Due to these five constraints one is left with two free parameters, ex.  $\tan \beta$  and  $m_A$ . It should be stressed that the soft breaking, in the Higgs sector, is actually encoded in this two-parameter freedom. (Indeed, if exact susy were imposed,  $V_{soft} = 0$ , then all  $\lambda_i$ ’s would be fixed in terms of the gauge couplings  $g, g'$ , together with  $\tan \beta = 1$  and  $m_A = 0$  [26] ). Subsequently, the presence (at the tree-level) of more than these two free parameters in the Higgs sector would be associated to the hard breaking of supersymmetry. The most

---

<sup>2</sup>quantum corrections should be consistently omitted here, as they contribute non-leading effects to the one-loop corrected  $e^+ e^- \rightarrow H^+ H^-$ , see also discussion in section 5

general parameterization of such a breaking leading back to the general THDM discussed in the previous section, can be cast in the form:

$$\begin{aligned}\lambda_1 &= \lambda_2 + \delta_{12} & , \quad \lambda_3 &= \frac{1}{8}(g^2 + g'^2) - \lambda_1 + \delta_{31} \\ \lambda_4 &= 2\lambda_1 - \frac{1}{2}g'^2 + \delta_{41} & , \quad \lambda_5 &= -\frac{1}{2}(g^2 + g'^2) + 2\lambda_1 + \delta_{51} \\ \lambda_6 &= -\frac{1}{2}(g^2 + g'^2) + 2\lambda_1 + \delta_{61}\end{aligned}\quad (15)$$

where the  $\delta$ 's measure the amount of hard breaking of supersymmetry.

The various Higgs masses and  $\tan 2\alpha$  can then be related to the  $\delta$ 's upon use of the above equations in conjunction with eq.(2-4) as,

$$\begin{aligned}\tan 2\alpha &= \tan 2\beta \frac{m_A^2 + m_Z^2 - v^2(\delta_{51} + \delta_{61} + 4\delta_{31})}{m_A^2 - m_Z^2 - v^2(-\delta_{51} + \delta_{61} + 4\delta_{31} + 4\frac{\tan^2\beta}{1-\tan^2\beta}\delta_{12})} \\ m_{H^\pm}^2 &= m_A^2 + m_W^2 + v^2(\delta_{41} - \delta_{61}) \\ m_H^2 + m_h^2 &= m_A^2 + m_Z^2 + v^2(4\delta_{31} + \delta_{51} - \delta_{61} - 4\sin^2\beta\delta_{12}) \\ m_H^2 - m_h^2 &= \sqrt{(\cos 2\beta(m_Z^2 - m_A^2 + v^2(-\delta_{51} + \delta_{61} + 4\delta_{31} + 4\frac{\tan^2\beta}{1-\tan^2\beta}\delta_{12})))^2(1 + \tan^2 2\alpha)}\end{aligned}\quad (16)$$

Now the crucial point is to note that the MSSM tree-level mass-sum-rules,

$$m_{H^0, h^0}^2 = \frac{1}{2}(m_Z^2 + m_A^2 \pm \sqrt{(m_Z^2 + m_A^2)^2 - 4m_Z^2 m_A^2 \cos^2 2\beta}) \quad (17)$$

$$m_{H^\pm}^2 = m_A^2 + m_W^2 \quad (18)$$

as well as

$$\tan 2\alpha = \tan 2\beta \frac{m_A^2 + m_Z^2}{m_A^2 - m_Z^2} \quad (19)$$

can be recovered *not only in the susy case*  $\delta'$ 's = 0, but *actually in a full one-parameter subspace*. Indeed the validity of eq.( 17-19 ) requires the following equations

$$\begin{aligned}\delta_{51} + \delta_{61} + 4\delta_{31} &= 0 & , \quad \delta_{61} - \delta_{51} + 4\delta_{31} + 4\frac{\tan^2\beta}{1-\tan^2\beta}\delta_{12} &= 0 \\ \delta_{41} - \delta_{61} &= 0 & , \quad 4\delta_{31} + \delta_{51} - \delta_{61} - 4\sin^2\beta\delta_{12} &= 0\end{aligned}\quad (20)$$

which are satisfied if

$$\begin{aligned}\delta_{12} &= \frac{(\tan^4\beta - 1)}{\tan^4\beta}\delta_{31} & , \quad \delta_{51} &= \frac{-2(1 + \tan^2\beta)}{\tan^2\beta}\delta_{31} \\ \delta_{61} &= \delta_{41} = \frac{2(1 - \tan^2\beta)}{\tan^2\beta}\delta_{31}\end{aligned}\quad (21)$$

With the above four constraints, we have just one extra free parameter as compared to the MSSM case, ex.  $\delta_{31}$  or equivalently  $\lambda_3$  eq.(15) on top of  $m_A$  and  $\tan\beta$ . Eqs.(21)

together with the set of free parameters  $(\lambda_3, m_A, \tan \beta)$ , define our quasi-susy (QSUSY) parameterization. Obviously, when  $\lambda_3$  hits its supersymmetric value, i.e. when  $\delta_{31} = 0$ , we get back the MSSM case, otherwise  $\Delta\lambda_3 = \lambda_3 - \lambda_3^{susy}$  can be seen as measuring the “hardness” of the susy breaking, while  $m_A$  and  $\tan \beta$  play the same role as in the MSSM.

There is a subtlety, however, as concerns the sign of  $\sin 2\alpha$ . Eqs.(21) are sufficient to lead to a looser constraint as compared to the well-known supersymmetric constraint [28]  $\sin 2\alpha < 0$ . Actually one can show that<sup>3</sup>

- a)  $\sin 2\alpha < 0$  can be chosen in all the parameter space;
- b)  $\sin 2\alpha > 0$  is possible provided  $\cos 2\alpha < 0$ ,  $\tan \beta < 1$  and  $m_A < m_Z$ ;

Case b) means that the only consistent choice becomes  $\sin 2\alpha < 0$  as soon as  $\tan \beta > 1$  or  $m_A > m_Z$ . Since in our study we assume a very heavy charged Higgs ( $m_{H^\pm} > 2m_Z$ ), thus a very heavy CP-odd neutral Higgs, eq.(18), we will stick to the choice  $\sin 2\alpha < 0$  throughout the paper. One can then determine uniquely the behavior of the various couplings in terms of  $\lambda_3, m_A, \tan \beta$ :

$$\begin{aligned} g_{H^0 H^+ H^-} &= g_{H^0 H^+ H^-}^{MSSM} - igm_W \left( \frac{1}{2c_w^2} + \frac{m_A^2}{m_W^2} + \frac{s_w^2}{\pi\alpha} \lambda_3 \right) \tan \beta \\ g_{h^0 H^+ H^-} &= g_{h^0 H^+ H^-}^{MSSM} - igm_W \frac{2m_A^2}{m_A^2 - m_Z^2} \left( \frac{1}{2c_w^2} + \frac{m_A^2}{m_W^2} + \frac{s_w^2}{\pi\alpha} \lambda_3 \right) \end{aligned} \quad (22)$$

where

$$\begin{aligned} g_{H^0 H^+ H^-}^{MSSM} &= -ig(m_W \cos(\beta - \alpha) - \frac{m_Z}{2c_w} \cos 2\beta \cos(\beta + \alpha)) \\ g_{h^0 H^+ H^-}^{MSSM} &= -ig(m_W \sin(\beta - \alpha) + \frac{m_Z}{2c_w} \cos 2\beta \sin(\beta + \alpha)) \\ g_{H^0 H^\pm G^\mp} &= \frac{-ig \sin(\beta - \alpha) (m_{H^\pm}^2 - m_H^2)}{2m_W} \\ g_{h^0 H^\pm G^\mp} &= \frac{ig \cos(\beta - \alpha) (m_{H^\pm}^2 - m_h^2)}{2m_W} \\ g_{A^0 H^\pm G^\mp} &= \mp \frac{m_{H^\pm}^2 - m_A^2}{2m_W} \end{aligned} \quad (23)$$

### 2.3 Charged Higgs-bosons interactions with gauge-bosons

The Higgs-bosons interactions with gauge-bosons are model independent. These interactions arise from the covariant derivatives in the Lagrangian:

$$\sum_i (D_\mu \Phi_i)^+ (D_\mu \Phi_i) = \sum_i [(\partial_\mu + ig \vec{T}_a \vec{W}_\mu^a + ig' \frac{Y_{\Phi_i}}{2} B_\mu) \Phi_i]^+ (\partial_\mu + ig \vec{T}_a \vec{W}_\mu^a + ig' \frac{Y_{\Phi_i}}{2} B_\mu) \Phi_i \quad (24)$$

---

<sup>3</sup> Detailed derivation of these and subsequent results related to QSUSY parameterization in the full Higgs sector including the leading one-loop corrections, will be given elsewhere

where:  $\vec{T}_a$  are the isospin gauge generators,  $Y_{\Phi_i}$  the hypercharge of the Higgs fields,  $W^a_\mu$  the  $SU(2)_L$  gauge fields,  $B_\mu$  the  $U(1)_Y$  gauge field, and  $g$  (resp.  $g'$ ) the associated coupling constants.

From eq. (24), one can easily extract the coupling of charged Higgs pair to the photon  $A_\mu$ , and Z boson  $Z_\mu$ . The corresponding Feynman rules read,

$$A_\mu H^+ H^- = -ie(p - p')_\mu \quad , \quad Z_\mu H^+ H^- = -ie \frac{c_W^2 - s_W^2}{2s_W c_W} (p - p')_\mu \quad (25)$$

Note that these vertices depend only on standard parameters (the electric charge and Weinberg angle). At tree-level, the  $H^\pm W^\mp A_\mu$  vertex does not exist as a consequence of the conservation of the electromagnetic current. On the contrary the vanishing of the  $H^\pm W^\mp Z_\mu$  vertex is accidental, (see [29] for further discussions). A consequence of the absence of these two vertices at tree-level is that the mixing  $H^\pm - W^\mp$  is not present in our study. From eq. (24) we can get also all the Feynman rules for the three and four point vertices involving Higgs and gauge bosons. Obviously all these Feynman rules have of the same structure in any THDM, irrespective of the implementation of supersymmetry, and depend only on the mixing angles  $\alpha$  and  $\beta$  (Appendix C). The only impact of SUSY there, as compared to a general THDM model, would be to require  $\sin 2\alpha \leq 0$ .

## 2.4 Charged Higgs-bosons interactions with fermions

In the two Higgs doublets extension of the standard model, there exist two different ways to couple Higgs fields to matter: either **type I** where the quarks and leptons couple exclusively to one of the two Higgs doublets, exactly as in the minimal standard model and will not be considered further in this paper, or the **type II** where, to avoid the problem of Flavor Changing Neutral Current (FCNC) [30],  $\Phi_1$  couples only to down quarks (and charged leptons) and  $\Phi_2$  couples only to up quarks (and neutral leptons). This latter model is the pattern found in the MSSM. In this case, the charged Higgs interaction to fermions is given by:

$$H^+ u \bar{d} = \frac{g V_{ud}}{\sqrt{2} m_W} \left( Y_U \frac{(1 - \gamma_5)}{2} + Y_D \frac{(1 + \gamma_5)}{2} \right) \quad (26)$$

where  $Y_U = \frac{m_U}{\tan \beta}$  and  $Y_D = \tan \beta m_D$ ,  $V_{ud}$  is the Kobayashi–Maskawa matrix element which we will take close to one.

## 3 Notations, conventions and cross section in the lowest order.

In this paper we will use the following notations and conventions. The momentum of the incoming electron and positron and outgoing Higgs bosons  $H^+$ ,  $H^-$  are denoted by  $p_1$ ,  $p_2$ ,  $k_1$  and  $k_2$ , respectively. Neglecting the electron mass  $m_e$  (and also the electron–Higgs

couplings which is proportional to  $m_e$ ), the momenta in the center-of-mass system of the  $e^+e^-$  are given by:

$$p_{1,2} = \frac{\sqrt{s}}{2}(1, 0, 0, \pm 1)$$

$$k_{1,2} = \frac{\sqrt{s}}{2}(1, \pm \kappa \sin \theta, 0, \pm \kappa \cos \theta)$$

where  $\sqrt{s}/2$  denotes the beam energy,  $\theta$  the scattering angle between the  $e^+$  and  $H^+$  flight directions in the laboratory frame,  $\kappa^2 = 1 - \frac{4m_{H^\pm}^2}{s}$ , and  $m_{H^\pm}$  the mass of the charged Higgs.

The Mandelstam variables are defined as follow:

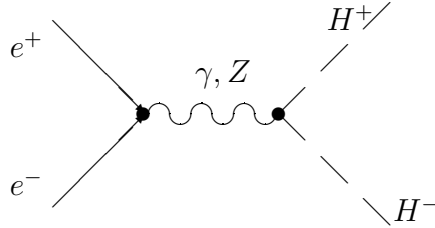
$$s = (p_1 + p_2)^2 = (k_1 + k_2)^2$$

$$t = (p_1 - k_1)^2 = (p_2 - k_2)^2 = m_{H^+}^2 - \frac{s}{2} + \frac{s}{2}\kappa \cos \theta$$

$$u = (p_1 - k_2)^2 = (p_2 - k_1)^2 = m_{H^+}^2 - \frac{s}{2} - \frac{s}{2}\kappa \cos \theta$$

$$s + t + u = 2m_{H^+}^2$$

The only Feynman diagrams contributing at the tree-level are the  $\gamma$  and  $Z$  s-channel exchange, [the electron–Higgs coupling being negligibly small, there is no t-channel contribution at this order.]



The contributions to the lowest-order amplitude have the following form:

$$\mathcal{M}_0^\gamma = -2\frac{e^2}{s}\bar{v}(p_2) k_1 u(p_1) \quad (27)$$

$$\mathcal{M}_0^Z = 2\frac{e^2 g_H}{s - m_z^2} (g_V \bar{v}(p_2) k_1 u(p_1) - g_A \bar{v}(p_2) k_1 \gamma^5 u(p_1)) \quad (28)$$

where  $g_V = (1 - 4s_W^2)/(4c_W s_W)$ ,  $g_A = 1/(4c_W s_W)$ ,  $g_H = -(c_W^2 - s_W^2)/(2c_W s_W)$ ,  $c_W \equiv \cos \theta_W$ ,  $s_W \equiv \sin \theta_W$ .

As one can see from eq. (27, 28), those amplitudes can be expressed in terms of two invariants,  $I_V$  and  $I_A$  defined as:

$$I_V = \bar{v}(p_2) k_1 u(p_1), \quad I_A = \bar{v}(p_2) k_1 \gamma^5 u(p_1) \quad (29)$$

The Born amplitude is given by:

$$\mathcal{M}_0 = \mathcal{M}_0^\gamma + \mathcal{M}_0^Z \quad (30)$$

From eqs. (27, 28), the corresponding differential cross section first studied in [21] is found to be,

$$\left( \frac{d\sigma}{d\Omega} \right)_0 = \frac{\alpha^2 \kappa^3}{8s} \left( 1 + g_H^2 \frac{g_V^2 + g_A^2}{(1 - m_Z^2/s)^2} - \frac{2g_H g_V}{1 - m_Z^2/s} \right) \sin^2 \theta \quad (31)$$

The total cross-section is:

$$\sigma_{tot} = \frac{\pi \alpha^2 \kappa^3}{3s} \left( 1 + g_H^2 \frac{g_V^2 + g_A^2}{(1 - m_Z^2/s)^2} - \frac{2g_H g_V}{1 - m_Z^2/s} \right) \quad (32)$$

At this stage we note the characteristic angular distribution of spin zero scalar particles which is expressed as:

$$\frac{2\pi}{\sigma_{tot}} \left( \frac{d\sigma}{d\Omega} \right)_0 = \frac{3}{4} \sin^2 \theta$$

This angular dependence leads to a vanishing forward–backward asymmetry  $A_{FB}$  at tree-level, where

$$A_{FB} = \frac{\int_{\theta \leq \pi/2} d\Omega \frac{d\sigma}{d\Omega} - \int_{\theta \geq \pi/2} d\Omega \frac{d\sigma}{d\Omega}}{\int_{\theta \leq \pi/2} d\Omega \frac{d\sigma}{d\Omega} + \int_{\theta \geq \pi/2} d\Omega \frac{d\sigma}{d\Omega}}$$

As we will see in the next section, at the one-loop level, only box diagrams can give contributions to  $A_{FB}$ .

## 4 Radiative corrections.

We have evaluated the radiative corrections at the one-loop level in the 't Hooft–Feynman gauge. These one-loop corrections are ultraviolet (UV) and infrared (IR) divergent. The UV singularities are treated by dimensional regularization in the on–mass–shell renormalization scheme while the IR singularities are regularized with a small fictitious photon mass  $m_\gamma$ . We renormalize not only the masses and coupling constants, but also the field wave functions in such a way that the residues of renormalized propagators are equal to one.

The typical Feynman diagrams for the virtual corrections of order  $\alpha^2$  are drawn in figure 1. These comprise, the THDM contribution to the photon and  $Z$  propagator and their mixing (Fig. 1.1), the standard contribution to the initial state (Fig. 1.2, 1.3 and 1.4), the THDM contribution to the final vertex (Fig. 1.5–1.12) and the THDM box contributions (Fig. 1.13 and 1.14). Because of their contributions to the forward–backward asymmetry, supersymmetric boxes (Fig. 1.15–1.18) will also be considered. The amplitudes of the Feynman diagrams depicted in Fig. 1.19 and Fig. 1.20 are proportional to the electron

mass and thus negligible. Bremsstrahlung diagrams and diagrams with a virtual photon emission are shown in Fig 1.21–1.30.

Those Feynman diagrams are generated and computed using FeynArts and FeynCalc packages [31] supplied with a full MSSM and THDM-II Feynman rules code [32]. We also used the Fortran FF-package [33], in the numerical analysis. The one loop amplitude  $\mathcal{M}^1$  projects fully on the two invariants defined in eq.(29) as

$$\mathcal{M}^1 = \mathcal{M}_A^1 I_A + \mathcal{M}_V^1 I_V \quad (33)$$

The typical one loop contributions are given in this form in terms of the Passarino–Veltman functions in appendix C and D.

We should note, by the way, that the supersymmetric box and vertex contributions involving  $\chi^+$  (resp.  $\chi^0$ ), and  $\tilde{\nu}$  (resp.  $\tilde{e}$ ) couplings to  $e^\pm$  lead to additional invariants, namely  $\bar{v}u$  and  $\bar{v}\gamma_5 u$ . These come with potentially sizeable effects from large supersymmetric partner masses, however, the chirality structure of the MSSM couplings combines to lead only contributions which vanish with the electron mass. Note also that one loop contributions coming from initial state  $e^+e^-H_0$  and  $e^+e^-h_0$  vertices are also vanishing like  $m_e$ , since  $e^+$  and  $e^-$  are both on-shell. A similar argument holds for the  $A^0$  and neutral goldstone exchange diagrams, as well as  $Z - A^0$  and  $Z - G^0$  mixing, noting also that  $A^0H^+H^-$  and  $G^0H^+H^-$  couplings are already forbidden at tree-level by  $CP$  invariance.

The diagrams of figure 1: 1.26–1.30 together with real Bremsstrahlung figure 1: 1.21–1.24 are needed to yield an IR finite corrected differential cross section which has the following form:

$$\left(\frac{d\sigma}{d\Omega}\right)_1 = \left(\frac{d\sigma}{d\Omega}\right)_0 + \left(\frac{d\sigma}{d\Omega}\right)_{SB} + 2\text{Re}(\mathcal{M}_0^* \mathcal{M}^1) \frac{\kappa}{64\pi^2 s} \quad (34)$$

Here  $\left(\frac{d\sigma}{d\Omega}\right)_{SB}$  denotes the soft Bremsstrahlung contribution. Using eqs. (27–30 and 33) the term  $\text{Re}(\mathcal{M}_0^* \mathcal{M}^1)$  reads:

$$\text{Re}(\mathcal{M}_0^* \mathcal{M}^1) = [\mathcal{M}_A^1 \left( -\frac{e^2 g_H g_A}{4(s - m_Z^2)} s^2 \kappa^2 \right) + \mathcal{M}_V^1 \left( \frac{e^2}{4} \kappa^2 (-s + s^2 \frac{g_H g_V}{(s - m_Z^2)}) \right)] \sin^2 \theta \quad (35)$$

As one can see from the last formula the interference term is proportional to  $\sin^2 \theta$ . Consequently, since vertex and self-energy contributions to  $\mathcal{M}_{A,V}^1$  have only  $s$  dependence, they will not contribute to the forward-backward asymmetry  $A_{FB}$ . Only box diagrams can contribute to  $A_{FB}$  through their  $t$  and  $u$  dependence.

Let us cast the various one-loop corrections in the form:

$$\sigma_1 = \sigma_0(1 + \delta) = \sigma_0(1 + \delta_{soft}^\gamma + \delta_{fermions} + \delta_{bosons} + \delta_{susy}^{boxes}) \quad (36)$$

where  $\delta_{soft}^\gamma$  is the soft photon contribution,  $\delta_{fermions}$  is the full vertex and self-energy contributions of all leptons and quarks,  $\delta_{bosons}$  the gauge boson and Higgs contributions in vertices self-energies and boxes. Finally  $\delta_{susy}^{boxes}$  designates the full box contributions from the supersymmetric sector. As we said before, this contribution will be considered only to illustrate the sensitivity of  $A_{FB}$  to various corrections.

## 4.1 On-mass-shell Renormalization.

The parameters entering the tree-level observables eqs.(31–32) are all standard model parameters, except for the charged Higgs mass itself. This fact will render the one-loop renormalization rather simple, in the sense that all non-standard parameters appearing first at the one-loop level, will not get renormalized. In particular, renormalization conditions related to the definition of  $\tan\beta$  are not explicitly needed here. We will need, however, to renormalize the charged Higgs wave-function and mass. On the other hand, the renormalization scheme should be chosen in such a way to allow a simple interpolation between the MSSM and the THDM-II. If we choose to renormalize  $m_{A^0}$  on-shell, identifying the pole of the propagator with the mass parameter in the renormalized Lagrangian  $\mathcal{L}_{\mathcal{R}}$ , then  $m_{H^\pm}$  would be uniquely determined in the MSSM, through the mass sum-rules, and its renormalized quantity would be shifted from the corresponding mass parameter in  $\mathcal{L}_{\mathcal{R}}$ , [8]. In the THDM-II case, one would then need to define, somewhat artificially, the renormalized  $m_{H^\pm}$  also to depart from the corresponding parameter in  $\mathcal{L}_{\mathcal{R}}$ , though in such a way that one recovers the MSSM situation when  $\lambda_i \rightarrow \lambda_i^{MSSM}$ . To avoid such complications, the simplest will be to take in the MSSM  $m_{H^\pm}$  as a free parameter (rather than  $m_{A^0}$ ) and renormalize it on-shell. This allows to treat the MSSM and THDM-II cases at equal footing in the charged Higgs sector, with a unique renormalization scheme.

We will adopt throughout, the renormalization scheme of refs. [34]–[35]. In this scheme one renormalizes all the fields before electroweak symmetry breaking. A renormalization constant  $Z_{\Phi_{1,2}}$  is introduced for each doublet  $\Phi_{1,2}$ ,  $Z_2^W$  for the  $SU_L(2)$  triplet  $W_\mu^a$  and  $Z_2^B$  for the  $U(1)$  singlet. The gauge fields, coupling constants and vacuum expectation values  $v_i$  are renormalized as follow:

$$\begin{aligned} W_\mu^a &\rightarrow (Z_2^W)^{1/2} W_\mu^a \\ B_\mu &\rightarrow (Z_2^B)^{1/2} B_\mu \\ \Phi_i &\rightarrow (Z_{\Phi_i})^{1/2} \Phi_i \\ g &\rightarrow (Z_1^W)(Z_2^W)^{-3/2} g \\ g' &\rightarrow (Z_1^B)(Z_2^B)^{-3/2} g' \\ v_i &\rightarrow (Z_{\Phi_i})^{1/2} (v_i - \delta v_i) \end{aligned} \tag{37}$$

In the on-mass-shell scheme the counterterms can be fixed by the following renormalization conditions:

- The on-shell conditions for  $m_W$ ,  $m_Z$ ,  $m_e$  and the electric charge  $e$  are defined as in the standard model [34].
- On-shell condition for the charged Higgs boson  $H^\pm$ : we choose to identify the physical charged Higgs mass with the corresponding parameter in  $\mathcal{L}_{\mathcal{R}}$ , and require the residue of the propagator to have its tree-level value, i.e.,

$$\delta m_{H^\pm}^2 = Re \sum^{H^+H^+} (m_{H^\pm}^2) \quad \text{and} \quad \delta Z^{H^\pm} = \frac{\partial}{\partial p^2} (\sum^{H^+H^+} (p^2))|_{p^2=m_{H^\pm}^2} \tag{38}$$

where  $\Sigma^{H^+H^+}(p^2)$  is the charged Higgs bare self-energy.

- Tadpoles are renormalized in such a way that the renormalized tadpoles vanish:  $T_h + \delta t_h = 0$ ,  $T_H + \delta t_H = 0$ . These conditions guarantee that  $v_{1,2}$  appearing in  $\mathcal{L}_{\mathcal{R}}$  are located at the minimum of the one-loop potential.

As we are looking for a charged Higgs bosons pair production and using  $m_{H^\pm}$  and  $\tan\beta$  as independent parameters (in the Higgs sector), we can choose a renormalization scheme very close to that of [35]. The main difference with [35] being that we renormalize the charged Higgs on-shell rather than the CP-odd  $A_0$ .

To compute the counterterms necessary to our study, we have to make all the substitutions given in eqs.(37) in the covariant derivative and replace the renormalization constants  $Z_i$  by their expansion up to first order,  $Z_i = 1 + \delta Z_i$ . Those transformations shift  $(D_\mu \Phi_i)^+(D_\mu \Phi_i)$  to the corresponding expression in terms of renormalized fields and couplings plus a set of counterterms. In our case we need just the two following ones:

$$\begin{aligned}\delta(A_\mu H^+ H^-) &= -ie[\delta Z^{H^\pm} + (\delta Z_1^\gamma - \delta Z_2^\gamma) + g_H(\delta Z_1^{\gamma z} - \delta Z_2^{\gamma z})](p+q)_\mu \\ \delta(Z_\mu H^+ H^-) &= ieg_H[\delta Z^{H^\pm} + (\delta Z_1^z - \delta Z_2^z) + \frac{1}{g_H}(\delta Z_1^{\gamma z} - \delta Z_2^{\gamma z})](p+q)_\mu\end{aligned}\quad (39)$$

where  $\delta Z^{H^\pm}$  is related to  $\delta Z_{\Phi_{1,2}}$  by the relation  $\delta Z^{H^\pm} = \sin^2\beta\delta Z_{\Phi_1} + \cos^2\beta\delta Z_{\Phi_2}$ , the  $\delta Z_i^\gamma$ ,  $\delta Z_i^z$  and  $\delta Z_i^{\gamma z}$  are related to  $\delta Z_i^W$  and  $\delta Z_i^B$  as in [35]<sup>4</sup>.

$$\begin{aligned}\delta Z_i^\gamma &= s_W^2 \delta Z_i^W + c_W^2 \delta Z_i^B \\ \delta Z_i^z &= c_W^2 \delta Z_i^W + s_W^2 \delta Z_i^B \\ \delta Z_i^{\gamma z} &= -c_W s_W (\delta Z_i^W - \delta Z_i^B) = \frac{-c_W s_W}{c_W^2 - s_W^2} (\delta Z_i^z - \delta Z_i^\gamma)\end{aligned}$$

Moreover, in the on-shell scheme defined in ref [34], the wave function renormalization constants of the gauge bosons are given by:

$$\delta Z_2^\gamma = -\frac{\partial \Sigma^\gamma}{\partial p^2}(0) \quad (40)$$

$$\delta Z_1^\gamma = \delta Z_2^\gamma + \frac{s_W}{c_W} \frac{\Sigma^{\gamma Z}(0)}{m_Z^2} \quad (41)$$

$$\delta Z_2^z = \delta Z_2^\gamma + 2 \frac{c_W^2 - s_W^2}{s_W c_W} \frac{\Sigma^{\gamma Z}(0)}{m_Z^2} + \frac{c_W^2 - s_W^2}{s_W^2} \left( \frac{\delta m_Z^2}{m_Z^2} - \frac{\delta m_W^2}{m_W^2} \right) \quad (42)$$

$$\delta Z_1^z = \delta Z_2^\gamma + \frac{3c_W^2 - 2s_W^2}{s_W c_W} \frac{\Sigma^{\gamma Z}(0)}{m_Z^2} + \frac{c_W^2 - s_W^2}{s_W^2} \left( \frac{\delta m_Z^2}{m_Z^2} - \frac{\delta m_W^2}{m_W^2} \right) \quad (43)$$

$$\delta Z_{1,2}^{\gamma, z} = -\frac{c_W s_W}{c_W^2 - s_W^2} (\delta Z_{1,2}^z - \delta Z_{1,2}^\gamma) \quad (44)$$

---

<sup>4</sup>note ,however, a difference in the convention for the sign of the Weinberg angle  $\theta_W$ .

Using these relations, one finds for the renormalization constants appearing in eq. (39):

$$\delta Z_1^\gamma - \delta Z_2^\gamma = \frac{s_W}{c_W} \frac{\Sigma^{\gamma Z}(0)}{m_Z^2} = -\frac{\alpha}{2} B_0(0, m_W^2, m_W^2) \quad (45)$$

$$\delta Z_1^Z - \delta Z_2^Z = \frac{c_W}{s_W} \frac{\Sigma^{\gamma Z}(0)}{m_Z^2} = -\frac{\alpha c_W^2}{2s_W^2} B_0(0, m_W^2, m_W^2) \quad (46)$$

$$\delta Z_1^{\gamma Z} - \delta Z_2^{\gamma Z} = -\frac{\Sigma^{\gamma Z}(0)}{m_Z^2} = \frac{\alpha c_W}{2s_W} B_0(0, m_W^2, m_W^2) \quad (47)$$

Note that the above combinations are independent of the fermion and charged Higgs contributions because  $\Sigma^{\gamma Z}(p^2)$  is vanishing at  $p^2 = 0$ .

The renormalization constant of the charged Higgs wave function is given by:

$$\delta Z^{H^\pm} = \delta Z_{bosons}^{H^\pm} + \delta Z_{fermions}^{H^\pm} \quad (48)$$

with:

$$\begin{aligned} \delta Z_{bosons}^{H^\pm} &= \frac{\alpha}{4\pi s_W^2} (2s_W^2 B_0(m_{H^\pm}^2, 0, m_{H^\pm}^2) + \frac{1}{2} B_0(m_{H^\pm}^2, m_A^2, m_W^2) + \frac{c_{\beta\alpha}^2}{2} B_0(m_{H^\pm}^2, m_h^2, m_W^2) \\ &+ \frac{s_{\beta\alpha}^2}{2} B_0(m_{H^\pm}^2, m_h^2, m_W^2) + \frac{(-1 + 2s_W^2)^2}{2c_W^2} B_0(m_{H^\pm}^2, m_{H^\pm}^2, m_Z^2) + 4m_{H^\pm}^2 B'_0(m_{H^\pm}^2, m_\gamma^2, m_{H^\pm}^2) \\ &+ \frac{1}{4} (2m_A^2 + 2m_{H^\pm}^2 - m_W^2 - 4g_{AH^+G^-}^2 s_W^2) B'_0(m_{H^\pm}^2, m_A^2, m_W^2) - g_{hH^+H^-}^2 B'_0(m_{H^\pm}^2, m_h^2, m_W^2) \\ &+ \frac{1}{4} (c_{\beta\alpha}^2 (2m_h^2 + 2m_{H^\pm}^2 - m_W^2) - 4g_{hH^+G^-}^2 s_W^2) B'_0(m_{H^\pm}^2, m_h^2, m_W^2) \\ &- g_{HH^+H^-}^2 B'_0(m_{H^\pm}^2, m_h^2, m_W^2) + \frac{1}{4} (s_{\beta\alpha}^2 (2m_h^2 + 2m_{H^\pm}^2 - m_W^2) \\ &- 4g_{HH^+G^-}^2 s_W^2) B'_0(m_{H^\pm}^2, m_h^2, m_W^2) + \frac{(4m_{H^\pm}^2 - m_Z^2)}{4c_W^2} (c_W^2 - s_W^2)^2 B'_0(m_{H^\pm}^2, m_{H^\pm}^2, m_Z^2)) \\ \delta Z_{fermions}^{H^\pm} &= \frac{N_C \alpha}{8\pi m_W^2 s_W^2} (-(Y_U^2 + Y_D^2) B_0(m_{H^\pm}^2, m_D^2, m_U^2) \\ &+ ((m_D^2 + m_U^2 - m_{H^\pm}^2)(Y_U^2 + Y_D^2) + 4m_D m_U Y_U Y_D) B'_0(m_{H^\pm}^2, m_D^2, m_U^2)) \end{aligned} \quad (49)$$

where  $\{c, s\}_{\beta\alpha} = \{\cos, \sin\}(\beta - \alpha)$ ,  $Y_U$  and  $Y_D$  are defined in eq. (26).  $N_C = 3$  for quarks and 1 for leptons. The couplings  $g_{AH^+G^-}$ ,  $g_{hH^+H^-}$ ,  $g_{HH^+H^-}$ ,  $g_{hH^+G^-}$  and  $g_{HH^+G^-}$  are trilinear scalar couplings which are model dependent.  $B'_0$  is the derivative of the  $B_0$  function with respect to the square of the charged Higgs 4-momentum taken at  $p_{H^\pm}^2 = m_{H^\pm}^2$ . In the above expressions, only  $B'_0(m_{H^\pm}^2, m_\gamma^2, m_{H^\pm}^2)$  contains infrared divergences, regulated here by  $m_\gamma$  which should cancel with the appropriate Bremsstrahlung contributions.

To sum up, most divergences (including initial state  $\gamma e^+e^-$  and  $Z e^+e^-$  vertices, and  $Z$  and  $\gamma$  self-energies and mixing) are absorbed in the renormalization of the standard parameters, the electric charge,  $M_Z, M_W, m_e$  and the wave functions, as usual. The one-loop correction to the  $H^\pm$  self-energy cancels out when the Higgs pair is produced on

shell. The only remaining non-standard renormalization is that of  $\gamma H^+ H^-$  and  $Z H^+ H^-$  vertices, given by eqs. (39). Furthermore, its model-dependence is exclusively contained in the charged Higgs wave function renormalization constant  $\delta Z^{H^\pm}$  as can be seen from eqs. (48, 49). Hence the renormalization procedure will involve essentially a set of (standard) parameters, which, combined with the quasi-susy parameterization of section 2, would facilitate a simultaneous treatment and comparison of THDM-II and MSSM cases.

## 4.2 Bremsstrahlung

In order to have an IR finite result we have to add to the cross section the contribution from  $e^+ e^- \rightarrow H^+ H^- \gamma$  in the soft-photon limit; the relevant diagrams are drawn in Fig. 1.21-1.30.

Denoting the photon four-momentum by  $k$  and its polarization vector by  $\epsilon_\mu(k)$  the amplitude of the soft Bremsstrahlung can be written in the form,

$$\begin{aligned} \epsilon_\mu \mathcal{M}_{SB}^\mu &= e \mathcal{M}_{Born} \left( \frac{p_1 \epsilon}{p_1 k} - \frac{p_2 \epsilon}{p_2 k} + \frac{k_2 \epsilon}{k_2 k} - \frac{k_1 \epsilon}{k_1 k} \right) \\ &\quad - 2e^3 \bar{v}(p_2) \not{e} \left( \frac{1}{s} + \frac{g_H(-g_V + g_A \gamma^5)}{s - m_z^2} \right) u(p_1). \end{aligned} \quad (50)$$

The differential cross section is as follows:

$$\begin{aligned} \left( \frac{d\sigma}{d\Omega} \right)_{SB} &= \left( \frac{d\sigma}{d\Omega} \right)_0 \delta_{SB} \\ &\quad + 8 \frac{\alpha^3}{s} \left( 1 - \frac{2g_V g_H}{1 - m_Z^2/s} + \frac{g_H^2(g_V^2 + g_A^2)}{(1 - m_Z^2/s)^2} \right) (I_0 - \frac{s}{4} \kappa^2 \sin^2 \theta (I_1 + I_2)) \end{aligned} \quad (51)$$

where  $\delta_{SB}$ ,  $I_0$ ,  $I_1$  et  $I_2$  are given by,

$$\begin{aligned} \delta_{SB} &= -e^2 \int_{k < \Delta E} \frac{d^3 k}{2\omega_k} \left\{ \frac{p_1}{p_1 k} - \frac{p_2}{p_2 k} + \frac{k_2}{k_2 k} - \frac{k_1}{k_1 k} \right\}^2 \\ I_{0,1,2} &= \frac{1}{\pi^2} \int \frac{d^3 k_1}{2\omega_{k_1}} \frac{d^3 k_2}{2\omega_{k_2}} \frac{d^3 k}{2\omega_k} (1, \frac{1}{k_1 k}, \frac{1}{k_2 k}) \end{aligned}$$

$\delta_{SB}$  can be expressed in terms of dilogarithms as:

$$\begin{aligned} \delta_{SB} &= -\frac{\alpha}{\pi} \left\{ 2 \ln \left( \frac{4\Delta E^2}{m_\gamma^2} \right) - \ln \left( \frac{4\Delta E^2}{m_\gamma^2} \right) \ln \left( \frac{s}{m_e^2} \right) + \ln \left( \frac{m_e^2}{s} \right) + \frac{1}{\beta} \ln \left( \frac{1-\beta}{1+\beta} \right) \right. \\ &\quad \left. + \frac{1+\beta^2}{2\beta} \ln \left( \frac{4\Delta E^2}{m_\gamma^2} \right) \ln \left( \frac{1-\beta}{1+\beta} \right) + 2 \ln \left( \frac{4\Delta E^2}{m_\gamma^2} \right) \ln \left( \frac{m_{H^+}^2 - u}{m_{H^+}^2 - t} \right) \right. \\ &\quad \left. + \frac{\pi^2}{3} + \frac{1}{2} \ln^2 \left( \frac{m_e^2}{s} \right) + \frac{1+\beta^2}{\beta} \left[ \text{Li}_2 \left( \frac{2\beta}{1+\beta} \right) + \frac{1}{4} \ln^2 \left( \frac{1-\beta}{1+\beta} \right) \right] \right\} \end{aligned}$$

$$\begin{aligned}
& +2 \left[ Li_2 \left( 1 - \frac{s(1-\beta)}{2(m_{H^+}^2 - t)} \right) + Li_2 \left( 1 - \frac{s(1+\beta)}{2(m_{H^+}^2 - t)} \right) \right. \\
& \left. - Li_2 \left( 1 - \frac{s(1-\beta)}{2(m_{H^+}^2 - u)} \right) - Li_2 \left( 1 - \frac{s(1+\beta)}{2(m_{H^+}^2 - u)} \right) \right] \} \quad (52)
\end{aligned}$$

In the soft-photon approximation for the Bremsstrahlung process  $e^+e^- \rightarrow H^+H^-\gamma$ , only photons with energies below the cut-off  $\Delta E \ll E$  are included. The infrared divergence is regulated by a fictitious small photon mass  $m_\gamma$ .

We have checked algebraically and numerically that  $m_\gamma$  cancels out when the Bremsstrahlung cross-section is added to the rest. Note also that the Sudakov effects  $\ln^2(m_e^2/s)$  cancel with the QED diagrams in the initial state.

Numerically, we find that the second term of the right-hand side of eq. (51) is very small compared to the term proportional to  $\delta_{S\mathcal{B}}$  and can be ignored.

## 5 Numerical analysis and discussion.

In this section we focus on the numerical analysis. We take the following experimental input for the physical parameters [36]:

- the fine structure constant:  $\alpha = \frac{e^2}{4\pi} = 1/137.03598$ .
- the mass of the gauge boson  $m_Z = 91.172 \text{ GeV}$ ,  $m_W = 80 \text{ GeV}$ .
- the input lepton masses:

$$m_e = 0.511 \text{ MeV} \quad m_\mu = 0.1057 \text{ MeV} \quad m_\tau = 1.784 \text{ GeV}$$

- for the light quark masses we use the effective values which are chosen in such a way that the experimentally extracted hadronic part of the vacuum polarizations is reproduced [37]:

$$\begin{aligned}
m_d &= 46 \text{ MeV} & m_u &= 46 \text{ MeV} & m_s &= 150 \text{ MeV} \\
m_c &= 1.5 \text{ GeV} & m_b &= 4.5 \text{ GeV} & &
\end{aligned}$$

In the on-shell scheme we consider,  $\sin^2 \theta_W$  is given by  $\sin^2 \theta_W \equiv 1 - \frac{m_W^2}{m_Z^2}$  valid beyond tree-level. The derived value  $\sin^2 \theta_W \simeq 0.23$  thus includes radiative corrections.

Fig.2 shows the integrated tree level cross section  $\sigma_0(f\text{b})$  as a function of charged Higgs mass  $m_{H^\pm}$  for three values of  $\sqrt{s}$ . It can be seen that for a charged Higgs mass around 220–230 GeV and for an integrated luminosity of about 10 to 50  $\text{fb}^{-1}$  (for the corresponding energy of 500 GeV), a few hundred events of charged Higgs pairs are expected at LC2000. We can have the same situation for higher c.m. energies (1 TeV–2 TeV), where the integrated luminosity is expected to be of about 200  $\text{fb}^{-1}$ , and for charged Higgs mass not very close to its threshold value.

We have listed in table 1 the contribution to the integrated cross section (in percent) and to the forward–backward asymmetry due to the soft–photon Bremsstrahlung and the virtual photon emission for several values of the soft–photon energy cut–off  $\Delta E$ . The dependence on  $\Delta E$  is rather important, for example, at  $\sqrt{s} = 500\text{GeV}$  and for  $m_{H^\pm} = 220\text{GeV}$  the correction increases from  $-11.2\%$  for  $\Delta E = 0.15E$  to reach  $-24.9\%$  at  $\Delta E = 0.05E$ . The forward–backward asymmetry is small.

We discuss now the contribution of fermions (light fermions and top–bottom) to the s–channel self-energy of the gauge bosons ( $\gamma\gamma$ ,  $\gamma Z$  and  $ZZ$ ) and to the  $\gamma H^+H^-$  and  $ZH^+H^-$  vertices. For more details on the effects of top–bottom contributions we refer the reader to ref [23]. Light fermion contributions are not very sensitive neither to  $\tan\beta$  nor to  $m_{H^\pm}$ . We have listed in table 2 some numerical values for the corrected total cross section (in percent) for several center of mass energies, charged Higgs mass and  $\tan\beta$ , the effects are rather small  $0.43\%–2.7\%$ . The top-bottom contribution is very sensitive to  $\tan\beta$  because of the form of the coupling given by eq.(26) which depends on the top–mass. For a top quark mass around  $180\text{ GeV}$  and for large  $\tan\beta = 30$ , we can reach a large correction, about  $-35\%$  at  $(\sqrt{s} = 500\text{GeV}, m_{H^\pm} = 220\text{GeV})$  and  $-25.7\%$  at  $(\sqrt{s} = 1500\text{GeV}, m_{H^\pm} = 680\text{GeV})$ . Total fermionic contribution is dominated by the top-bottom contribution.

To discuss the contribution of the bosonic sector (Higgs bosons and gauge bosons contribution) to the initial  $ee\gamma$  and  $eeZ$  vertices, the gauge boson self energy, the final state vertex and the box contributions<sup>5</sup>, we will use the QSUSY parameterization described in section II. This parameterization allows a comparison between the MSSM and THDM-II and is described only by three parameters  $m_{H^\pm}$ ,  $\tan\beta$  and  $\lambda_3$ .

In Fig 3–5 we show the percentage contribution to the integrated cross section as a function of  $\sqrt{s}$  and for different values of  $\lambda_3$  and  $\tan\beta$ . One finds that when  $\lambda_3$  takes its supersymmetric value  $\lambda_3^{MSSM}$  the bosonic contribution is moderate (for both small and large  $\tan\beta$ ) and increases with increasing c.m. energy, reaching  $10\%$  for  $\sqrt{s} \approx 2\text{TeV}$  and for a charged Higgs mass lower than  $430\text{ GeV}$ . This correction interferes destructively with the fermionic contribution. Thus we can conclude that in the MSSM and for large  $\tan\beta$  large effects exceeding  $10\%$  contribution.

For charged Higgs mass of about  $730\text{ GeV}$  (Fig 5.a and 5.b) and if  $\lambda_3$  takes its supersymmetric value  $\lambda_3^{MSSM}$  the bosonic contribution is very small (about  $3\%$ ).

If we take  $\lambda_3$  away from its supersymmetric value, the situation changes drastically. For a small deviation from  $\lambda_3^{MSSM}$  the effect is still of the same order as in the MSSM. Far from  $\lambda_3^{MSSM}$  and both for  $\tan\beta = 2$  and  $\tan\beta = 30$  one can find large correction  $30\%–40\%$  which can cancel those of the top–bottom found in the case of large  $\tan\beta$ .

Note that contributions from the initial  $e^+e^-\gamma$ ,  $(Z)$  vertices to the corrected cross section are of order  $0.44\%$  at  $\sqrt{s} = 500\text{GeV}$ ,  $1.3\%$  at  $\sqrt{s} = 1000\text{GeV}$  and  $1.83\%$  at  $\sqrt{s} = 1500\text{GeV}$ .

As one can see from the Fig 3–5, for a convenient choice of  $\sqrt{s}$ ,  $m_{H^\pm}$ ,  $\tan\beta$  and  $\lambda_3$  one can find positive correction to the total cross section which can cancel the negative fermionic contribution. Fig.6, 6.a and 6. b are to illustrate those positive effects which are shown to increase with  $\tan\beta$ .

---

<sup>5</sup>Note that soft photon contributions have been subtracted and are given separately in table 1.

The standard boxes are not sensitive to  $\tan\beta$ , but can give important contributions. For instance:

- at  $\sqrt{s} = 500\text{GeV}$  the effect is about 4.7% for a Higgs mass of  $110\text{ GeV}$  and 3.5% for a Higgs mass of  $320\text{ GeV}$ .
- at  $\sqrt{s} = 1000\text{GeV}$  the effect is about 6.5% for a Higgs mass of  $230\text{ GeV}$  and 5.4% for a Higgs mass of  $410\text{ GeV}$ .
- at  $\sqrt{s} = 1500\text{GeV}$  the effect is about 7.6% for a Higgs mass of  $410\text{ GeV}$  and 6.5% for a Higgs mass of  $680\text{ GeV}$ .

Fig. 7 shows the one-loop forward-backward asymmetry  $A_{FB}$  as a function of  $\sqrt{s}$ . As one can see from this figure,  $A_{FB}$  is small in both cases: MSSM or THDM-II; this is the consequence of the fact that the  $A_{FB}$  is generated only from box diagrams, the couplings there being independent of  $\lambda_3$ . We have computed also the supersymmetric boxes depicted in figure 1. (1.15–1.18) The SUSY boxes amplitudes are given in the appendix D. We have listed in table 3 some numerical values for the SUSY boxes (corrected cross section in percent and the contribution to the  $A_{FB}$ ) for several choices of the sleptons masses and charginos and neutralinos mass. The  $A_{FB}$  is small and the corrected cross section is found small and negative.

The total cross section  $\sigma_1(fb)$  is plotted in figures 8 and 9 for two values of  $m_{H^\pm}$  and  $\tan\beta$  and for various choices of  $\lambda_3$ . Shown is the summed effect of all fermionic and bosonic contributions, excluding the gauge invariant set of diagrams containing at least one virtual photon exchange [the numerical contribution of the latter being mainly that of the IR sector]. In all cases we have illustrated, the one loop cross section is smaller than the tree level cross section  $\sigma_0(fb)$ .

## 6 Conclusion

Future  $e^+e^-$  linear colliders will probably offer the cleanest environment to discover a heavy charged Higgs through pair production. We have calculated the corresponding one loop radiative corrections within the THDM-II and the MSSM using the on-mass-shell scheme, concentrating mainly here on the model-dependent contributions of the Higgs sector as well as the model-independent soft photon contributions. We also introduced the QSUSY parameterization which allows a practical comparison between the two models and involves only one extra parameter (ex.  $\lambda_3$ ) as compared to the MSSM. The soft photon contribution for this process is found to be substantial (about -20%) for moderate values of the soft-photon energy cut-off  $\Delta E$ . If  $\lambda_3$  takes its MSSM values the contribution of the Higgs sector turns out to be rather small (a few percent). In this case large effects can still come from the top-bottom/stop-sbottom apart from (non-generic) possible cancellations studied elsewhere [23]. Away from its MSSM values,  $\lambda_3$  induces large and positive effects which can cancel the negative effects coming from top-bottom contribution, both for small and large  $\tan\beta$ . Those large corrections arise from the contributions of model-dependent vertices

(A.10–A.11) which enter both the final state vertex and the charged Higgs renormalization constant. We also illustrated the overall sensitivity to the charged Higgs mass,  $\tan\beta$  and the c.m. energy.

In summary, the radiative corrections to the charged Higgs pair production in  $e^+e^-$  annihilation can be significant and should be included in any reliable analysis. Furthermore, the large model-dependent effects can help discriminate phenomenologically between a (softly broken) supersymmetric and a non-supersymmetric minimal Higgs sector, irrespective of direct evidence for the susy spectrum.

**Acknowledgment:** We thank Michel Capdequi Peyranère for his critical reading of the manuscript and also for his collaboration in the early stage of this work.

AA acknowledges a research grant from Camões Institut of Lisbonne and thanks the Departamento de Fisica–Centra, Instituto Superior Tecnico for the worm hospitality during his visit where part of this work has been done.

## Table Captions:

**Tab. 1:** Soft photon contributions to the corrected cross section (in percent) and to the forward–backward asymmetry with the following cut-off on the photon energy:

$$\Delta E_1 = 0.05\sqrt{s}/2, \Delta E_2 = 0.1\sqrt{s}/2, \Delta E_3 = 0.15\sqrt{s}/2$$

**Tab. 2:** Fermionic (leptons+light quarks+top–bottom) contributions to the corrected cross section (in percent) for  $m_{top} = 180 \text{ GeV}$ .

**Tab. 3:** SUSY boxes contributions to the corrected cross section (in percent) and to the forward–backward asymmetry

## Figure Captions:

**Fig. 1:** Feynman diagrams relevant for the  $\mathcal{O}(\alpha)$  contributions to  $e^+e^- \rightarrow H^+H^-$ . 1. 1) s-channel self energy diagrams, 1.2–1.4) s-channel initial state vertex diagrams, 1.5–1.12) s-channel final state vertex diagrams, 1.13–1.14) THDM-II boxes diagrams, 1.15–1.19) SUSY boxes diagrams, 1.21–1.25 Bremsstrahlung diagrams, 1.26–1.30) diagrams with a virtual photon and 1.31–1.35) self energy of the charged Higgs bosons necessary for the counterterms.

**Fig. 2:** Integrated tree level cross section as a function of  $m_{H^\pm}$  for three value of  $\sqrt{s} = 500 \text{ GeV}, 1000 \text{ GeV}$  and  $1500 \text{ GeV}$ .

**Fig. 3:** Bosonic contribution (not including virtual and soft–photon emission) to the integrated cross section as a function of  $\sqrt{s}$  for  $m_{H^\pm} = 220 \text{ GeV}$ , 3.a)  $\tan\beta = 2$  and severals values for  $\lambda_3$ , 3.b)  $\tan\beta = 30$  and severals values for  $\lambda_3$

**Fig. 4:** Same as in Fig.3 with  $m_{H^\pm} = 420 \text{ GeV}$

**Fig. 5:** Same as in Fig.3 with  $m_{H^\pm} = 730 \text{ GeV}$

**Fig. 6:** Bosonic contribution (in percent) to the integrated cross section as a function of  $\tan\beta$ , a)  $m_{H^\pm} = 220 \text{ GeV}, \sqrt{s} = 500 \text{ GeV}$  and different choices for  $\lambda_3$ , b)  $m_{H^\pm} = 300 \text{ GeV}, \sqrt{s} = 1000 \text{ GeV}$  and different choices for  $\lambda_3$ , c)  $m_{H^\pm} = 420 \text{ GeV}, \sqrt{s} = 1000 \text{ GeV} \dots$

**Fig. 7:** Standard box contributions to forward–Backward asymmetry as function of  $\sqrt{s}$  with  $m_{H^\pm} = 220 \text{ GeV}, \tan\beta = 2$  and for several values of  $\lambda_3$  around  $\lambda_3^{MSSM}$

**Fig. 8:** Total one loop cross section  $\sigma_1$  (in  $fb$ ) as a function of  $\sqrt{s}$  for  $m_{top} = 180 \text{ GeV}$  and  $m_{H^\pm} = 220 \text{ GeV}$ , 8. a)  $\tan\beta = 2, \lambda_3 = \lambda_3^{MSSM} = -0.72, \lambda_3 = -1.2$  and  $\lambda_3 = 0.05$ , 8. b)  $\tan\beta = 30, \lambda_3 = \lambda_3^{MSSM} = -0.72, \lambda_3 = -0.84$  and  $\lambda_3 = -0.8$ .

**Fig. 9:** Total one loop cross section  $\sigma_1$  (in  $fb$ ) as a function of  $\sqrt{s}$  for  $m_{top} = 180 \text{ GeV}$  and  $m_{H^\pm} = 420 \text{ GeV}$ , 9. a)  $\tan\beta = 2, \lambda_3 = \lambda_3^{MSSM} = -2.71, \lambda_3 = -3.6$  and  $\lambda_3 = -1.8$ , 9. b)  $\tan\beta = 30, \lambda_3 = \lambda_3^{MSSM} = -2.71, \lambda_3 = -2.9$  and  $\lambda_3 = -2.62$ .

## References

- [1] H.E. Haber and G.L. Kane, Phys. Rep. 117 (1985) p75.  
H.P. Nilles, Phys. Rep. **110** (1984) 1;  
P. Nath, R. Arnowitt and A. Chamseddine, “Applied N=1 Supergravity”, ITCP Series in Theoretical Physics, World Scientific, Singapore 1984;  
X.R. Tata, in Proceedings of the “Mt Sorak Symposium on the Standard Model and Beyond”, Mt Sorak, Korea, 1990;
- [2] J.P. Derendinger and C.A. Savoy, N. Phys. **B237** (1984) 307, J. Ellis, J.F. Gunion, H.E. Haber, L. Roszkowski, F. Zwirner, Phys. Rev. D39 (1989) 844, U. Ellwanger, M. Rausch de Traubenberg, Z. Phys. **C53** (1992) 521
- [3] J.L. Feng, M.E. Peskin, H. Murayama, X. Tata Phys.Rev. **D52**, (1995) p1418-1432.
- [4] H.E.Haber and R.Hempfling, Phys. Rev. Lett. **66** , (1991), p1815.  
Y.Okada, M.Yamaguchi and T.Yanagida, Prog. Theor. Phys. Lett. **85**, (1991) p1.  
J.Ellis, G.Ridolfi and F.Zwirner, Phys.Lett. **B257** (1991) p83.  
for further references see the talk by F.Zwirner, CERN-TH-6792-93.
- [5] M. Carena, M. Quiros and C. E. M. Wagner, Nucl. Phys. **B461**, (1996), p407.  
H. E. Haber, R. Hempfling and A. H. Hoang, Z. Phys. **C75** (1997) p539.
- [6] J.F. Gunion, A. Turski Phys.Rev. **D40**: 2333, 1989; J.F. Gunion, A. Turski Phys.Rev. **D39** : 2701, 1989.
- [7] D. M. Pierce, J. A. Bagger, K. T. Matchev, and R-J Zhang, Nucl. Phys. **B491**, (1997), p3.
- [8] A.Brignole et al., Phys.Lett. **B271** (1991) 123; B273 (1991) 550(E);  
M.A.Diaz and H.E.Haber, Phys.Rev. **D45** (1992) 4246;  
P.H.Chankowski, S.Pokorski and J.Rosiek, Phys.Lett.**B274** (1992) 191;  
A.Brignole, Phys.Lett. **B277** (1992) 313;
- [9] R. A. Jimenez, J. Sola, Phys. Lett. **B389**, (1996) p53.  
A. Bartl, H. Eberl, K. Hidaka, T. Kon, W. Majerotto and Y. Yamada, Phys.Lett. **B378**, (1996), p167.
- [10] K. Ackerstaff et al, The OPAL Collaboration, Phys.Lett. **B426** (1998) p180. P. Abreu et al, DELPHI Collaboration Phys.Lett. **B420** (1998) p140 and R. Barate et al, ALEPH Collaboration, Phys.Lett. **B418** (1998) p419.
- [11] F. Abe et al, CDF Collaboration Phys.Rev.Lett. **79**: (1997) p357; *ibid.*, Phys. Rev. **D54**, (1996) p735; *ibid.*, Phys. Rev. Lett. **73** (1996) p2667.

- [12] D.P. Roy *hep-ph* 9704442, presented at the 32nd Rencontres de Moriond , M. Guchait and D.P. Roy, *Phys. Rev.* **D55**, (1997), p7263; CDF Collaboration (F. Abe et al.) *Phys.Rev.Lett.* **79**: 357-362, 1997 (hep-ex/9704003)
- [13] F. M. Borzumati and A. Djouadi *hep-ph* 9806301 and references therein.
- [14] T.G. Rizzo, *Phys. Rev.* **D 38** (1988) 820; W.-S. Hou and R.S. Wiley, *Phys. Lett.* **B 302** (1988) 591; C.Q. Geng and J.N. Ng, *Phys. Rev.* **D 38** (1988) 2857; V. Barger, J.L. Hewet and R.J.N. Phillips, *Phys. Rev.* **D 41** (1990) 269.
- [15] M. Ciuchini, G. Degrassi, P. Gambino and G.F. Giudici *hep-ph/9710335*; F. M. Borzumati and C. Greub, *hep-ph/9802391*;
- [16] T. Goto , Y. Okada, *Prog.Theor.Phys.Suppl.*123 (1996) **213**; and *Prog.Theor.Phys.* **94** (1995) 407.
- [17] Jiang Yi et al *Journ. Phys* **G23** (1997) p325, *G24* (1998) p83, S. S. D. Willenbrock, *Phys. Rev.* **D35** (1987) p173 and A. Krause, T. Plehn, M. Spira and P. M. Zerwas, *Nucl.Phys.* B519 (1998) 85-100
- [18] V. Barger and R.J.N. Phillips, *Phys. Rev.* **D41**, (1990) p884; A. C. Bawa, C.S. Kim and A. D. Martin, *Z. Phys.* **C47**, (1990) p75; R.M. Godbole and D.P. Roy *Phys. Rev.* **D43**, (1991) p3640; M. Drees and D.P. Roy *Phys. Lett.* **B269**, (1991) p155.
- [19] V. Barger, R.J.N. Phillips and D. P. Roy, *Lett.* **B324**, (1994) p236; J. F. Gunion, H. E. Haber, F. E. Paige, W. K. Tung and S. S. D. Willenbrock, *Nucl. Phys.* **B294**, 621 (1987); R. M Barnet, H. E. Haber and D. E. Soper, *Nucl. Phys.* B306, (1988) p697; F. I. Olness and W. K. Tung, *Nucl. Phys.* **B308**, (1988) p813. J. L. Diaz-Cruz and O. A. Sampayo, *Phys. Rev.* **D50**, (1994) p6820 S. Moretti and K. Odagiri, *Phys. Rev.* **D55**, (1997) p5627
- [20] D. A. Dicus, J. L. Hewett, C. Kao and T. G. Rizzo, *Phys. Rev.* **D40** (1989) p787 A. A. Barrientos Bendezú and B. A. Kniehl, MPI/PhT/98-054 *hep-ph/9807480*
- [21] S. Komamiya, *Phys. Rev.* **D38** (1988) 2158;
- [22] A. Arhrib, M. Capdequi Peyranère, W. Hollik and G. Moultaka in preparation
- [23] A. Arhrib, M. Capdequi Peyranère and G. Moultaka, *Phys. Lett.* **B341**, p313–324, (1995); Marco A. Diaz and Tonnis A. ter Veldhuis, *hep-ph/9501315*, DPF94 proceedings;
- [24] A. Arhrib, G. Moultaka Proceedings of the Physics with  $e^+e^-$  Linear Colliders Workshop, Annecy–Gran Sasso–Hamburg 1995, ed. P. Zerwas (*hep-ph/9606300*).

- [25] D. Bowser-Chao et al, Phys. Lett. **B315** (1995) p 313; W. G. Ma et al Phys. Rev. **D53** (1996) p1304 and Shou Hua Zhu, Chong Sheng Li and Chong Shou Gao hep-ph/9712367.
- [26] J. F. Gunion and H. E. Haber, Nucl.Phys. **B272** (1986) 1 and ERRATA hep-ph/9301205;
- [27] H. Komatsu and J. Kubo, Phys. Lett. **B157** (1985) 90; Nucl. Phys. **B263** (1986) 265;
- [28] J. F. Gunion and H. E. Haber, Nucl. Phys. **B278**: 449, 1986 and ERRATA hep-ph/9301205;
- [29] For a review see e.g. J.F. Gunion, H.E. Haber, G.L. Kane and S. Dawson, The Higgs hunter's guide (Addison-Wesley, Redwood City, 1990) and ERRATA SCIPP-92/58 (Dec. 92)
- [30] S.Glashow et S.Weinberg, Phys.Rev. **D15** (1977) p1958.
- [31] H.Eck and J. Kublbeck, Guide to FeynArts 1.0, University of Wurzburg, 1992.  
R.Mertig, Guide to FeynCalc 1.0, University of Wurzburg, 1992.
- [32] A.Arhrrib, thesis , University Montpellier II(1994) Unpublished;
- [33] G.J. van Oldenborgh, Comput.Phys.Commun. **66** (1991) 1;
- [34] M.Böhm, W.Hollik and H.Spiesberger, Fortschr.Phys.**34** (1986) 11;
- [35] A. Dabelstein and W. Hollik MPI-PH-93-86, Contributed to Workshop on e+ e- Collisions at 500 GeV: the Physics Potential. Published in SUSY 94 Workshop:109-118 A. Dabelstein Z.Phys. **C67**,(1995), p495 and P. Chankowski, S. Pokorski and J. Rosiek Nucl.Phys.**B423**: 437-496,(1994)
- [36] OPAL Collaboration. Phys.Lett. **B370** (1996) p174 and R. M. Barnett et al. Phys. Rev. **D54** (1996) p1.
- [37] H. Burkhardt, F. Jegerlehner, G. Penso et C. Verzegnassi, Z. Phys. **C43** (1989) 497.  
F. Jegerlehner, in Proc. 1990. Theoretical advanced study institute in elementary particle physics, eds. M. Cvetic and P. Langacker, World scientific, Singapore (1991) 476. and *hep-ph*: 9502298.  
A. D. Martin and D. Zeppenfeld Phys. Lett **B345** (1995), p558
- [38] A. Denner, H. Eck, O. Hahn, J. Kublbeck Nucl.Phys.**B387**, (1992), p467
- [39] A. Dabelstein Z.Phys.**C67**,(1995), p495 and P. Chankowski, S. Pokorski and J. Rosiek Nucl.Phys.**B423**: 437-496,(1994)
- [40] W. Hollik and C. Schappacher, KA-TP-3-1998 hep-ph/9807426

$\sqrt{s}$	500GeV		1 TeV		1.5 TeV	
$m_{H^+} GeV$	170	220	300	420	500	680
$\delta_{soft}^\gamma(\Delta E_1)(\%)$	-26.4	-24.9	-28.3	-26.8	-28.7	-26.9
$\delta_{soft}^\gamma(\Delta E_2)(\%)$	-17.5	-16.3	-18.8	-17.7	-19.2	-17.6
$\delta_{soft}^\gamma(\Delta E_3)(\%)$	-12.3	-11.2	-13.3	-12.3	-13.5	-12.1
$A_{FBsoft}^\gamma(\Delta E_1)$	0.034	0.016	0.125	0.029	-0.020	0.0066
$A_{FBsoft}^\gamma(\Delta E_2)$	0.023	0.0120	0.0709	0.0212	-0.0184	0.0053
$A_{FBsoft}^\gamma(\Delta E_3)$	0.0199	0.00997	0.0527	0.0172	-0.0172	0.0046

**Table 1.**

$\sqrt{s}$	500GeV		1 TeV		1.5 TeV	
$(m_{H^+} GeV, \tan\beta)$	(170,2)	(220,2)	(300, 2)	(420,2)	(500,2)	(680,2)
$\delta_{light-fermions} (\%)$	2.55	2.54	2.64	2.64	2.73	2.73
$\delta_{top-bottom} (\%)$	-11.	-18.9	-11.8	-12.8	-9.95	-14.4
$\delta_{total-fermions} (\%)$	-8.44	-16.4	-9.1	-10.1	-7.21	-11.7
$(m_{H^+} GeV, \tan\beta)$	(170,10)	(220,10)	(300, 10)	(420,10)	(500,10)	(680,10)
$\delta_{light-fermions} (\%)$	2.40	2.34	2.49	2.46	2.60	2.48
$\delta_{top-bottom} (\%)$	-8.50	-11.25	-7.71	-8.02	-6.67	-7.95
$\delta_{total-fermions} (\%)$	-6.10	-8.91	-5.22	-5.56	-4.07	-5.47
$(m_{H^+} GeV, \tan\beta)$	(170,20)	(220,20)	(300,20)	(420,20)	(500,20)	(680,20)
$\delta_{light-fermions} (\%)$	1.96	1.69	2.04	1.92	2.15	1.71
$\delta_{top-bottom} (\%)$	-10.3	-20.	-11.8	-12.9	-9.96	-14.4
$\delta_{total-fermions} (\%)$	-8.33	-18.4	-9.73	-10.9	-7.81	-12.7
$(m_{H^+} GeV, \tan\beta)$	(170,30)	(220,30)	(300, 30)	(420,30)	(500,30)	(680,30)
$\delta_{light-fermions} (\%)$	1.22	0.61	1.28	1.01	1.40	0.42
$\delta_{top-bottom} (\%)$	-13.4	-35.2	-18.8	-21.2	-15.7	-25.7
$\delta_{total-fermions} (\%)$	-12.2	-34.6	-17.5	-20.2	-14.2	-25.2

**Table 2.**

$M = 300, M' = 250, \mu = -120, m_{\tilde{e}_L} = 460, m_{\tilde{e}_R} = 390, m_{\tilde{\nu}} = 340 \text{ (GeV)}$						
$\sqrt{s}$	500GeV		1 TeV		1.5 TeV	
$(\tan\beta, m_{H^\pm})$	(02, 180)	(40, 220)	(02, 300)	(40, 420)	(02, 500)	(40, 680)
$\delta_{susy}^{boxes} (\%)$	-0.20	-0.28	-5.32	-2.8	-9.	-2.63
$A_{FB}$	0.0068	0.011	-0.036	-0.025	-0.052	-0.017

$M = 500, M' = 400, \mu = -300, m_{\tilde{e}_L} = 600, m_{\tilde{e}_R} = 550, m_{\tilde{\nu}} = 540 \text{ (GeV)}$						
$\sqrt{s}$	500GeV		1 TeV		1.5 TeV	
$(\tan\beta, m_{H^\pm})$	(10, 180)	(40, 220)	(10, 300)	(40, 420)	(10, 500)	(40, 680)
$\delta_{susy}^{boxes} (\%)$	-0.34	-0.28	-1.9	-2.31	-4.19	-14.3
$A_{FB}$	$-.7310^{-4}$	-0.00028	0.001	.00086	-.024	-.085

$M = 220, M' = 180, \mu = -400, m_{\tilde{e}_L} = 230, m_{\tilde{e}_R} = 220, m_{\tilde{\nu}} = 210 \text{ (GeV)}$						
$\sqrt{s}$	500GeV		1 TeV		1.5 TeV	
$(\tan\beta, m_{H^\pm})$	(15, 180)	(40, 220)	(15, 300)	(40, 420)	(10, 500)	(40, 680)
$\delta_{susy}^{boxes} (\%)$	-1.08	-1.12	-6.54	-11.06	-11.6	-34.2
$A_{FB}$	-0.0029	-0.005	-0.039	-0.057	-0.069	-0.18

**Table 3.**

# Appendix

## Appendix A: Couplings

For completeness, we give in this section the Feynman rules of the 3-point vertices involving the charged Higgs in the general THDM, in two different forms.

In terms of the  $\lambda_i$ 's,  $\alpha$  and  $\beta$ , one has

$$\begin{aligned} g_{H^0 H^+ H^-} &= -i\sqrt{2}v\left[-\frac{\lambda_5}{2} \sin 2\beta \sin(\alpha + \beta) + (\lambda_4 + 2\lambda_3) \cos(\beta - \alpha) \right. \\ &\quad \left. + \sin 2\beta (\lambda_2 \sin \alpha \cos \beta + \lambda_1 \cos \alpha \sin \beta)\right] \end{aligned} \quad (\text{A.1})$$

$$\begin{aligned} g_{h^0 H^+ H^-} &= -i\sqrt{2}v\left[-\frac{\lambda_5}{2} \sin 2\beta \cos(\alpha + \beta) + (\lambda_4 + 2\lambda_3) \sin(\beta - \alpha) \right. \\ &\quad \left. + \sin 2\beta (\lambda_2 \cos \alpha \cos \beta - \lambda_1 \sin \alpha \sin \beta)\right] \end{aligned} \quad (\text{A.2})$$

$$\begin{aligned} g_{H^0 H^\pm G^\mp} &= -\frac{iv}{\sqrt{2}}\left[(\lambda_5 - \lambda_4) \cos 2\beta \sin(\alpha + \beta) + \lambda_4 \sin 2\beta \cos(\alpha + \beta) \right. \\ &\quad \left. + 2 \sin 2\beta (\lambda_2 \sin \alpha \sin \beta - \lambda_1 \cos \alpha \cos \beta)\right] \\ &= \frac{-ig \sin(\beta - \alpha)(m_{H^\pm}^2 - m_H^2)}{2m_W} \end{aligned} \quad (\text{A.3})$$

$$\begin{aligned} g_{h^0 H^\pm G^\mp} &= -\frac{iv}{\sqrt{2}}\left[(\lambda_5 - \lambda_4) \cos 2\beta \cos(\alpha + \beta) - \lambda_4 \sin 2\beta \sin(\alpha + \beta) \right. \\ &\quad \left. + 2 \sin 2\beta (\lambda_2 \cos \alpha \sin \beta + \lambda_1 \sin \alpha \cos \beta)\right] \\ &= \frac{ig \cos(\beta - \alpha)(m_{H^\pm}^2 - m_h^2)}{2m_W} \end{aligned} \quad (\text{A.4})$$

$$g_{A^0 H^\pm G^\mp} = \mp \frac{v}{\sqrt{2}} (\lambda_6 - \lambda_4) = \mp \frac{m_{H^\pm}^2 - m_A^2}{v\sqrt{2}} \quad (\text{A.5})$$

where the trigonometric functions of  $\alpha$  should be expressed further in terms of the  $\lambda_i$ 's and  $\tan \beta$ , using eqs.(3,4) with

$$v_1 = \frac{v}{\sqrt{1 + \tan \beta^2}} \quad v_2 = v \sqrt{\frac{\tan \beta^2}{(1 + \tan \beta^2)}}$$

Another useful form is in terms of deviations from the MSSM tree-level mass-sum-rules. Defining

$$\lambda_3 = \frac{1}{8}(g^2 + g'^2) - \lambda_1 + \frac{m_W^2}{v^2} \delta_3 \quad (\text{A.6})$$

$$m_{H^\pm}^2 = (m_{H^\pm}^2)_{MSSM} + m_W^2 \delta_\pm \quad (\text{A.7})$$

$$m_H^2 = (m_H^2)_{MSSM} + m_W^2 \delta_H \quad (A.8)$$

$$m_h^2 = (m_h^2)_{MSSM} + m_W^2 \delta_h \quad (A.9)$$

where  $(m_{H^\pm}^2)_{MSSM}$  and  $(m_{H/h}^2)_{MSSM}$  are given by eqs.(17, 18), then the Feynman rules for the vertices  $H_0 H^+ H^-$  and  $h_0 H^+ H^-$  read

$$\begin{aligned} g_{H^0 H^+ H^-} &= g_{H^0 H^+ H^-}^{MSSM} - i g m_W [\cos(\beta - \alpha) (\delta_\pm - \frac{\delta_H}{2}) + \\ &\quad \frac{\sin(\alpha + \beta)}{\sin 2\beta \tan^2 \beta} \{4\delta_3 - \frac{1}{2}(\delta_H + \delta_h) - \frac{1}{2 \cos^3 \beta} (\cos(2\alpha + \beta) + \\ &\quad \sin \beta (\frac{\sin 2\alpha}{2} + \sin(\alpha - \beta) \cos(\alpha + \beta))) (\delta_H - \delta_h)\}] \end{aligned} \quad (A.10)$$

$$\begin{aligned} g_{h^0 H^+ H^-} &= g_{h^0 H^+ H^-}^{MSSM} - i g m_W [\sin(\beta - \alpha) (\delta_\pm - \frac{\delta_H}{2}) + \\ &\quad \frac{\cos(\alpha + \beta)}{\sin 2\beta \tan^2 \beta} \{4\delta_3 - \frac{1}{2}(\delta_H + \delta_h) - \frac{1}{2 \cos^3 \beta} (\cos(2\alpha + \beta) + \\ &\quad \sin \beta (\frac{\sin 2\alpha}{2} + \sin(\alpha + \beta) \cos(\alpha - \beta))) (\delta_H - \delta_h)\}] \end{aligned} \quad (A.11)$$

It's interesting to note that in the general THDM the big effects (in the case where  $\tan \beta$  is large or very small) comes from the  $\delta_3$  or  $\delta_{H,h}$  but never from  $\delta_\pm$ . Note also that these effects are not present not only in the susy case but also when  $\delta_H = \delta_h = 4\delta_3$ .

## Appendix B: Passarino–Veltman Functions

Let us recall the definitions of scalar and tensor integrals we use: The inverse of the propagators are denoted by

$$D_0 = q^2 - m_0^2, \quad D_i = (q + p_i)^2 - m_i^2$$

One point functions:

$$A_0(m_0^2) = \frac{1}{i\pi^2} \int d^n q \frac{1}{D_0}$$

Two point functions:

$$B_{0,\mu}(p_1^2, m_0^2, m_1^2) = \frac{1}{i\pi^2} \int d^n q \frac{1, q_\mu}{D_0 D_1}$$

using Lorentz invariance, we have:

$$B_\mu = p_{1\mu} B_1$$

Three point functions:

$$C_{0,\mu,\mu\nu}(p_1^2, p_{12}^2, p_2^2, m_0^2, m_1^2, m_2^2) = \frac{1}{i\pi^2} \int d^n q \frac{1, q_\mu, q_\mu q_\nu}{D_0 D_1 D_2}$$

using Lorentz invariance, we have:

$$C_\mu = p_{1\mu} C_1 + p_{2\mu} C_2 \quad (\text{B.1})$$

$$C_{\mu\nu} = g_{\mu\nu} C_{00} + p_{1\mu} p_{1\nu} C_{11} + p_{2\mu} p_{2\nu} C_{22} + (p_{1\mu} p_{2\nu} + p_{2\mu} p_{1\nu}) C_{12} \quad (\text{B.2})$$

Four point functions:

$$D_{0,\mu,\mu\nu}(p_1^2, p_{12}^2, p_{23}^2, p_2^2, p_3^2, p_{13}^2, m_0^2, m_1^2, m_2^2, m_3^2) = \frac{1}{i\pi^2} \int d^n q \frac{1, q_\mu, q_\mu q_\nu}{D_0 D_1 D_2 D_3}$$

using Lorentz invariance, we have:

$$D_\mu = p_{1\mu} D_1 + p_{2\mu} D_2 + p_{3\mu} D_3 \quad (\text{B.3})$$

$$\begin{aligned} D_{\mu\nu} = & g_{\mu\nu} D_{00} + p_{1\mu} p_{1\nu} D_{11} + p_{2\mu} p_{2\nu} D_{22} + p_{3\mu} p_{3\nu} D_{33} + (p_{1\mu} p_{2\nu} + p_{2\mu} p_{1\nu}) D_{12} \\ & + (p_{1\mu} p_{3\nu} + p_{3\mu} p_{1\nu}) D_{13} + (p_{3\mu} p_{2\nu} + p_{2\mu} p_{3\nu}) D_{23} \end{aligned} \quad (\text{B.4})$$

## Appendix C: Vertex amplitudes.

In this section we give only some typical amplitudes of the final state vertex contributions drawn in figure 1. The amplitude will be projected on the two invariants  $I_V$  and  $I_A$  defined in section 3.

The s-channel self-energy  $\gamma\gamma$ ,  $\gamma Z$  and  $ZZ$  can be found in [39], [40] The standard model initial state vertex contributions Fig 1.2, 1.3 and 1.4 are well known and will not be given here.

The remaining amplitudes are given as follow:

### Diagram 1.5

$$\begin{aligned} \mathcal{M}_{1.5} = & \frac{\alpha^2 g_{SH^+W^-} g_{SH^-W^+} g_{VW^+W^-}}{s(s - m_V^2)\kappa^2} \left( -\frac{s}{m_{H^+}^2}(m_S^2 - m_W^2)\kappa^2 B_0(0, m_S^2, m_W^2) - \right. \\ & \left. \frac{1}{m_{H^+}^2}(8m_{H^+}^2[m_S^2 + m_{H^+}^2 - m_W^2] - m_S^2 s - 5m_{H^+}^2 s + m_W^2 s) B_0(m_{H^+}^2, m_S^2, m_W^2) \right) \end{aligned}$$

$$\begin{aligned}
& -2(-2m_S^2 + 2m_{H^+}^2 + 2m_W^2 + s)B_0(s, m_W^2, m_W^2) \\
& + (4m_S^4 - 8m_S^2m_{H^+}^2 + 4m_{H^+}^4 - 8m_S^2m_W^2 - 8m_{H^+}^2m_W^2 + 4m_W^4 - 8m_{H^+}^2s + \\
& 4m_W^2s + s^2)C_0(m_{H^+}^2, m_{H^+}^2, s, m_W^2, m_S^2, m_W^2) \Big) (g_V I_V - g_A I_A) \tag{C.1}
\end{aligned}$$

Where  $g_{ZW^+W^-} = \frac{c_W}{s_W}$ ,  $g_{\gamma W^+W^-} = 1$ ,  $g_{H_0 H^\mp W^\pm} = \pm \frac{1}{2s_W} s_{\beta\alpha}$ ,  $g_{h_0 H^\mp W^\pm} = \mp \frac{1}{2s_W} c_{\beta\alpha}$ ,  $g_{A_0 H^\mp W^\pm} = \frac{-i}{2s_W}$ , with  $\{c, s\}_{\beta\alpha} = \{\cos, \sin\}(\beta - \alpha)$  and  $\kappa^2 = 1 - \frac{4m_{H^\pm}^2}{s}$  and  $m_S$  is the mass of the scalar particle S.

## Diagram 1.6

$$\begin{aligned}
\mathcal{M}_{1.6} = & \frac{\alpha^2 g_{VSS'} g_{V'S_i H^-} g_{V'S_j H^+}}{m_{H^\pm}^2 s(s - m_V^2) \kappa^2} \Big( 2(s - 4m_{H^\pm}^2)(m_{V'}^2 - m_{S_j}^2)B_0(0, m_{V'}^2, m_{S_j}^2) \\
& + 2(s - 4m_{H^\pm}^2)(m_{V'}^2 - m_{S_i}^2)B_0(0, m_{V'}^2, m_{S_i}^2) \\
& - 2(m_{H^\pm}^2(6m_{S_j}^2 + 2m_{S_i}^2 + 8m_{H^\pm}^2 - 6m_{V'}^2 - 5s) + s(m_{V'}^2 - m_{S_j}^2))B_0(m_{H^\pm}^2, m_{S_j}^2, m_{V'}^2) \\
& - 2(m_{H^\pm}^2(2m_{S_j}^2 + 6m_{S_i}^2 + 8m_{H^\pm}^2 - 6m_{V'}^2 - 5s) + s(m_{V'}^2 - m_{S_i}^2))B_0(m_{H^\pm}^2, m_{S_i}^2, m_{V'}^2) \\
& + 8m_{H^\pm}^2(m_{S_j}^2 + m_{S_i}^2 + 2m_{H^\pm}^2 - m_{V'}^2 - 2s)B_0(s, m_{S_j}^2, m_{S_i}^2) \\
& - 2m_{H^\pm}^2 \Big( (m_{S_j}^2 + m_{S_i}^2)^2 + 4m_{H^\pm}^2(m_{S_j}^2 + m_{S_i}^2 + m_{H^\pm}^2) - 3(m_{V'}^2 + s)(m_{S_j}^2 + m_{S_i}^2) + \\
& m_{V'}^2(-6m_{H^\pm}^2 + 2m_{V'}^2 + 5s) - 6m_{H^\pm}^2s + 2s^2 \Big) [C_0(m_{H^\pm}^2, m_{H^\pm}^2, s, m_{S_i}^2, m_{V'}^2, m_{S_j}^2) \\
& C_0(m_{H^\pm}^2, m_{H^\pm}^2, s, m_{S_j}^2, m_{V'}^2, m_{S_i}^2)] \Big) (g_V I_V - g_A I_A) \tag{C.2}
\end{aligned}$$

the coupling constants being defined in the following table.

$(S, S', V')$	$(H_0, A_0, W^+)$	$(h_0, A_0, W^+)$	$(H^+, H^-, Z)$	$(H^-, H^-, \gamma)$
$g_{ZSS'}$	$i \frac{s_{\beta\alpha}}{2s_W c_W}$	$-i \frac{c_{\beta\alpha}}{2s_W c_W}$	$-\frac{(c_W^2 - s_W^2)}{2s_W c_W}$	$-\frac{(c_W^2 - s_W^2)}{2s_W c_W}$
$g_{\gamma SS'}$	0	0	-1	-1
$g_{H^\mp SV'}$	$\pm \frac{1}{2s_W} s_{\beta\alpha}$	$\mp \frac{1}{2s_W} c_{\beta\alpha}$	$-\frac{(c_W^2 - s_W^2)}{2s_W c_W}$	-1
$g_{H^\pm S'V'}$	$\frac{-i}{2s_W}$	$\frac{-i}{2s_W}$	$-\frac{(c_W^2 - s_W^2)}{2s_W c_W}$	-1

When  $V'$  is the photon, one has to keep consistently a photon mass regulator in  $C_0(m_{H^\pm}^2, m_{H^\pm}^2, s, m_{H^\pm}^2, m_{H^\pm}^2, m_{V'}^2)$  to account for the IR singularity, taking everywhere else in eq.(C.2)  $m_{V'} \rightarrow 0$ .

## Diagram 1.7 + 1.8

In this case: if  $V$  is the Z boson then  $V'$  is the Z boson (resp.  $W^\pm$  boson) and  $S_i$  is a neutral (resp. charged) Higgs boson while  $S_j$  is the charged (resp. neutral) one.

if  $V$  is the photon then  $V'$  is the  $W^\pm$  gauge boson and  $S_i$  is a charged Higgs boson while  $S_j$  is the neutral one.

$$\mathcal{M}_{1.7+1.8} = \frac{\alpha^2 g_{S_i S_j H^+} g_{V' S_j H^-} g_{V' S_i}}{s(s - m_V^2) \kappa^2} \left( 2B_0(m_{H^\pm}^2, m_{S_i}^2, m_{S_j}^2) + 2B_0(m_{H^\pm}^2, m_{S_j}^2, m_{V'}^2) - 4B_0(s, m_{S_i}^2, m_{V'}^2) + (m_{S_i}^2 - 6m_{H^\pm}^2 - 2m_{S_j}^2 + m_{V'}^2 + s)(C_0(m_{H^\pm}^2, m_{H^\pm}^2, s, m_{S_i}^2, m_{S_j}^2, m_{V'}^2) + C_0(m_{H^\pm}^2, m_{H^\pm}^2, s, m_{V'}^2, m_{S_j}^2, m_{S_i}^2)) \right) (g_V I_V - g_A I_A) \quad (\text{C.3})$$

$(S_i, S_j, V')$	$(H_0, H^+, Z)$	$(h_0, H^+, Z)$	$(G^+, H_0, W^\pm)$	$(G^+, h_0, W^\pm)$	$(G^+, A_0, W^\pm)$
$g_{ZV'S_i}$	$m_Z \frac{c_{\beta\alpha}}{s_W c_W}$	$m_Z \frac{s_{\beta\alpha}}{s_W c_W}$	$-m_Z s_W$	$-m_Z s_W$	$-m_Z s_W$
$g_{\gamma V' S_i}$	0	0	$m_W$	$m_W$	$m_W$
$g_{S_i S_j H^\mp}$	$-ig_{H_0 H^+ H^-}$	$-ig_{h_0 H^+ H^-}$	$-ig_{G^+ H_0 H^-}$	$-ig_{G^+ h_0 H^-}$	$ig_{A^0 G^\pm H^\mp}$
$g_{V' S_j H^\pm}$	$-\frac{(c_W^2 - s_W^2)}{2s_W c_W}$	$-\frac{(c_W^2 - s_W^2)}{2s_W c_W}$	$\pm \frac{1}{2s_W} s_{\beta\alpha}$	$\mp \frac{1}{2s_W} c_{\beta\alpha}$	$-i \frac{1}{2s_W}$

Where the coupling  $g_{H_0 H^+ H^-}$ ,  $g_{h_0 H^+ H^-}$ ,  $g_{H_0 H^+ G^-}$  and  $g_{h_0 H^+ G^-}$  are model dependent and are given in eqs. (A.10,A.11).

## Diagram 1.9

For this kind of diagram, we add to diagram 1. i another diagram with permutation of  $S_i$  and  $S_j$  in order to have symmetric amplitude.

In the case of three different scalar  $S_i$ ,  $S_j$  and  $S_k$  with  $S_i \neq S_j$ , only the Z boson is coupled to two different scalar (the coupling of the photon is forbidden because of the conservation of the electromagnetic current )

$$\mathcal{M}_{1.9} = \frac{\alpha^2 g_{H^+ S_j S_k} g_{H^- S_i S_k} g_{V' S_i S_j}}{s(s - m_V^2) \kappa^2} \left( 4B_0(m_{H^\pm}^2, m_{S_j}^2, m_{S_k}^2) + 4B_0(m_{H^\pm}^2, m_{S_i}^2, m_{S_k}^2) - 8B_0(s, m_{S_j}^2, m_{S_i}^2) + 2(m_{S_j}^2 + 2m_{H^\pm}^2 + m_{S_i}^2 - 2m_{S_k}^2 - s)(C_0(m_{H^\pm}^2, m_{H^\pm}^2, s, m_{S_i}^2, m_{S_k}^2, m_{S_j}^2) + C_0(m_{H^\pm}^2, m_{H^\pm}^2, s, m_{S_j}^2, m_{S_k}^2, m_{S_i}^2)) \right) (g_V I_V - g_A I_A) \quad (\text{C.4})$$

$(S_i, S_j, S_k)$	$(H_0, A_0, G^+)$	$(h_0, A_0, G^+)$
$g_{Z S_i S_j}$	$i \frac{s_{\beta\alpha}}{2s_W c_W}$	$-i \frac{c_{\beta\alpha}}{2s_W c_W}$
$g_{H^\pm S_j S_k}$	$ig_{A^0 G^\mp H^\pm}$	$ig_{A^0 G^\mp H^\pm}$
$g_{H^- S_i S_k}$	$-ig_{H_0 H^- G^+}$	$-ig_{h_0 H^- G^+}$

In the case of identical scalar  $S_i = S_j$  the amplitude can be deduced from the above one eq. (C.4) by setting  $m_{S_i} = m_{S_j}$  and multiplying by 1/2. We have the following situation: If  $S_i = H^+$  then  $V = \gamma$  or  $Z$ ,  $S_k = H_0$  or  $h_0$  in this case we have  $g_{ZH^+H^-} = -\frac{(c_W^2 - s_W^2)}{2s_W c_W}$ ,  $g_{\gamma H^+H^-} = -1$ . The coupling  $g_{H_0 H^+H^-}$  and  $g_{h_0 H^+H^-}$  are model dependent and are given in eqs. (A.10,A.11).

If  $S_i = G^+$  then  $V = \gamma$  or  $Z$ ,  $S_k = H_0, h_0$  or  $A_0$  in this case we have  $g_{ZG^+G^-} = -\frac{(c_W^2 - s_W^2)}{2s_W c_W}$ ,  $g_{\gamma G^+G^-} = -1$ .

## Diagram 1.10 and 1.11

The amplitude of diagram 1.10 is equal to the amplitude of 1.11.

$$\begin{aligned} \mathcal{M}_{1.10+1.11} = & \frac{\alpha^2 g_{VV'SH} - g_{SH^+V'}}{2(s - m_V^2)} ((m_S^2 - m_{V'}^2) B_0(0, m_S^2, m_{V'}^2) \\ & + (-m_S^2 - 3m_{H^\pm}^2 + m_{V'}^2) B_0(m_{H^\pm}^2, m_S^2, m_{V'}^2)) (g_V I_V - g_A I_A) \end{aligned} \quad (C.5)$$

Where  $V$  denotes the photon or the  $Z$  gauge boson,

$V'$  a charged (resp. neutral) gauge boson and  $S$  a neutral (resp. charged) scalar particle.

The couplings of these contributions are given by:

- $W^- H_0$  exchange:

$$\begin{aligned} V = \text{photon}, \quad g_{\gamma W^- H_0 H^+} &= -\frac{1}{2s_W} s_{\beta\alpha}, \quad g_{H_0 H^\mp W^\pm} = \pm \frac{1}{2s_W} s_{\beta\alpha} \\ V = Z, \quad g_{ZW^+ H_0 H^-} &= \frac{1}{2c_W} s_{\beta\alpha} \end{aligned}$$

- $W^- h_0$  exchange:

$$\begin{aligned} V = \text{photon}, \quad g_{\gamma W^+ h_0 H^-} &= \frac{1}{2s_W} c_{\beta\alpha}, \quad g_{h_0 H^\mp W^\pm} = \mp \frac{1}{2s_W} c_{\beta\alpha} \\ V = Z, \quad g_{ZW^+ h_0 H^-} &= -\frac{1}{2c_W} c_{\beta\alpha} \end{aligned}$$

- $W^- A_0$  exchange:

$$\begin{aligned} V = \text{photon}, \quad g_{\gamma W^+ A_0 H^-} &= \frac{-i}{2s_W}, \quad g_{A_0 H^\mp W^\pm} = \frac{-i}{2s_W} \\ V = Z, \quad g_{ZW^+ A_0 H^-} &= \frac{i}{2c_W} \end{aligned}$$

- $Z H^+$  exchange:

$$\begin{aligned} V = \text{photon}, \quad g_{\gamma Z H^+ H^-} &= \frac{c_W^2 - s_W^2}{s_W c_W}, \quad g_{\gamma H^+ H^-} = -1 \\ V = Z, \quad g_{ZZ H^+ H^-} &= \frac{(c_W^2 - s_W^2)^2}{2s_W^2 c_W^2}, \quad g_{ZH^+ H^-} = -\frac{c_W^2 - s_W^2}{2s_W c_W} \end{aligned}$$

- photon  $H^+$  exchange:

$$V = \text{photon}, g_{\gamma\gamma H^+ H^-} = 2, g_{\gamma H^+ H^-} = -1$$

$$V = Z, g_{\gamma Z H^+ H^-} = \frac{c_W^2 - s_W^2}{s_W c_W}, g_{\gamma H^+ H^-} = -1$$

## Diagram 1.12

For up-up-down exchange in the vertex the amplitude is given by:

- photon exchange:

$$\mathcal{M}_{1.12} = \frac{N_C \alpha^2}{m_W^2 s_W^2 s} \left( e_U (Y_U^2 + Y_D^2) B_0(s, m_U^2, m_U^2) + 2e_U (m_D^2 Y_U^2 + 2m_U m_D Y_U Y_D + m_D^2 Y_D^2) C_0(m_{H^\pm}^2, m_{H^\pm}^2, s, m_U^2, m_D^2, m_U^2) + 2e_U ((m_D^2 + m_{H^\pm}^2 + m_U^2) (Y_U^2 + Y_D^2) + 4m_D m_U Y_U Y_D) C_{11}(m_{H^\pm}^2, s, m_{H^\pm}^2, m_D^2, m_U^2, m_U^2) \right) I_V \quad (\text{C.6})$$

- Z-exchange:

$$\mathcal{M}_{1.12} = \frac{-N_C \alpha^2}{2c_W m_W^2 (s - m_V^2) s_W^3} \left( (2e_U s_W^2 (Y_U^2 + Y_D^2) - Y_D^2) B_0(s, m_U^2, m_U^2) + \{4e_U s_W^2 ((Y_U^2 + Y_D^2) m_D^2 + 2m_U m_D Y_U Y_D) - 2m_U m_D Y_U Y_D - 2m_D^2 Y_D^2\} C_0(m_{H^\pm}^2, m_{H^\pm}^2, s, m_U^2, m_D^2, m_U^2) - 2\{(m_U Y_U + m_D Y_D)^2 + m_{H^\pm}^2 Y_D^2 - 2e_U s_W^2 ((Y_U^2 + Y_D^2) (m_D^2 + m_{H^\pm}^2 + m_U^2) + 4m_D m_U Y_U Y_D)\} C_{11}(m_{H^\pm}^2, s, m_{H^\pm}^2, m_D^2, m_U^2, m_U^2) \right) (g_V I_V - g_A I_A) \quad (\text{C.7})$$

The contributions of the down-down-up vertex are obtained from the ones above through the replacement:

$$e_U \rightarrow -e_D, Y_U \rightarrow Y_D, Y_D \rightarrow Y_U, m_U \rightarrow m_D, m_D \rightarrow m_U$$

## Appendix D: Boxes amplitudes.

In this section we give the box amplitudes both for standard and supersymmetric cases.

### THDM-II boxes

We give the general amplitude for THDM-II boxes which are drawn in figure 1 ( 1.13, 1.14, 1.28, 1.29 and 1.30 ) with exchange of two gauge boson one scalar and one fermion. We denote by  $V_1$  and  $V_2$  the two gauge bosons with masses  $m_2$  and  $m_4$ ,  $S$  a scalar particle with

mass  $m_1$  and  $l$  a lepton (electron or neutrino) with mass  $m_3$  of which we keep trace only in the arguments of the Passarino-Veltman functions, and neglect otherwise.

We will use the following notations for the coupling:

- gauge boson–two scalars:  $V_\mu S_1 S_2 = i e g_H (p - p')_\mu$
- gauge boson–two fermions:  $V_\mu^i f f' = i e \gamma_\mu (g_{V_i} - g_{A_i} \gamma_5)$

we find then:

$$\mathcal{M}_{box} = \alpha^2 g_{H_1} g_{H_2} (GA \ I_A - GV \ I_V) \ INV$$

with :

$$GA = g_{A_2} g_{V_1} + g_{A_1} g_{V_2}, \quad GV = g_{A_1} g_{A_2} + g_{V_1} g_{V_2}$$

and

$$\begin{aligned} INV = & 4 C_0(m_e^2, m_e^2, s, m_2^2, m_3^2, m_4^2) - 2 C_0(m_e^2, m_{H^\pm}^2, t, m_3^2, m_4^2, m_1^2) + \\ & C_0(m_{H^\pm}^2, m_{H^\pm}^2, s, m_2^2, m_1^2, m_4^2) + 2(m_{H^\pm}^2 + 2m_1^2 - m_2^2 - t) D_0 + \\ & 2(m_{H^\pm}^2 + t) D_1 + 2(m_{H^\pm}^2 + t) D_2 + 2(m_{H^\pm}^2 - s + t) D_3 - \\ & C_1(m_{H^\pm}^2, s, m_{H^\pm}^2, m_1^2, m_2^2, m_4^2) - C_2(m_{H^\pm}^2, s, m_{H^\pm}^2, m_1^2, m_2^2, m_4^2) \end{aligned}$$

The  $D_0$  et  $D_{1i}$   $i = 1, 2, 3$  have as arguments  $(m_{H^\pm}^2, m_e^2, m_e^2, m_{H^\pm}^2, t, s, m_1^2, m_2^2, m_3^2, m_4^2)$ .

In the case of exchange of neutral gauge bosons in the box, we have to add the crossed boxes. The amplitude can be deduced from the above one by changing  $t$  into  $u$ .

In the case of photon exchange in the box we have to regularize the I.R divergence by a small mass. we have checked numerically and analytically that the I.R divergence cancels out when adding the soft photon Bremsstrahlung.

## Supersymmetric boxes

In this case we have two other invariants which contribute to the amplitude ( $\bar{v}(p_2)u(p_1)$  and  $\bar{v}(p_2)\gamma_5 u(p_1)$ ). In the limit of vanishing electron mass the coefficient of these two additional invariants are suppressed.

Boxes 1.16 and 1.17 contain lepton number violating vertices, we treat them using rules of reference [38].

### Box 1.16

$$\mathcal{M}_{2.d} = -\frac{\alpha^2}{2} g_{H^+ \tilde{e}_L \tilde{\nu}}^2 \sum_{i=1}^2 g_{e \chi_i^+ \tilde{\nu}}^L (I_A + I_V)(D_0 + D_1 + D_2 + D_3) \quad (D.1)$$

Where  $g_{H^+ \tilde{e}_L \tilde{\nu}} = -\frac{m_W}{s_W \sqrt{2}} \sin 2\beta$ ,  $g_{e \chi_i^+ \tilde{\nu}}^L = -\frac{V_{i1}}{s_W}$ ,

With

$$D_m \equiv D_m(m_{H^\pm}^2, m_e^2, m_e^2, m_{H^\pm}^2, u, s, m_{\tilde{e}_L}^2, m_{\tilde{\nu}}^2, m_{\chi_i^+}^2, m_{\tilde{\nu}}^2)_{m=0,\dots,3}$$

We are in the case of vanishing electron mass, then the coupling of the charged Higgs which is proportional to  $m_e$  is neglected.

### Box 1.15

$$\mathcal{M}_{2.c} = \frac{\alpha^2}{2} g_{H^+ \tilde{e}_L \tilde{\nu}}^2 \sum_{i=1}^4 g_{e \chi_i^0 \tilde{e}_L}^L (I_A + I_V)(D_0 + D_1 + D_2 + D_3) \quad (D.2)$$

$g_{e \chi_i^0 \tilde{e}_L}^L = \sqrt{2}(N'_{i1} + \frac{1}{s_W c_W}(1/2 - s_W^2)N'_{i2})$  Where the  $N'$  are defined in [26].

With

$$D_m(m_{H^\pm}^2, m_e^2, m_e^2, m_{H^\pm}^2, t, s, m_{\tilde{\nu}}^2, m_{\tilde{e}_L}^2, m_{\chi_i^0}^2, m_{\tilde{e}_L}^2)_{m=0,\dots,3}$$

### Box 1.18

We give first contributions from boxes involving virtual  $\tilde{e}_L$  exchange:

$$\begin{aligned} \mathcal{M}_{1.18L} = & -\frac{\alpha^2}{2} \sum_{i=1}^4 \sum_{j=1}^2 \sum_{k=1}^4 [(g_{e \chi_i^0 \tilde{e}_L}^L g_{e \chi_k^0 \tilde{e}_L}^L g_{H^+ \chi_i^0 \chi_j^-}^R g_{H^- \chi_k^0 \chi_j^+}^R)((m_{\chi_j^+}^2 + m_{\tilde{e}_L}^2 - t)D_0 + \\ & C_0[m_{H^\pm}^2, m_{H^\pm}^2, s, m_{\chi_i^0}^2, m_{\chi_j^+}^2, m_{\chi_k^0}^2] + (m_{\chi_j^+}^2 - t)(D_1 + D_2 + D_3)) \\ & + [m_{\chi_j^+} m_{\chi_k^0} g_{e \chi_i^0 \tilde{e}_L}^L g_{e \chi_k^0 \tilde{e}_L}^L g_{H^+ \chi_i^0 \chi_j^-}^R g_{H^- \chi_k^0 \chi_j^+}^L \\ & + m_{\chi_j^+} m_{\chi_i^0} g_{e \chi_i^0 \tilde{e}_L}^L g_{e \chi_k^0 \tilde{e}_L}^L g_{H^+ \chi_i^0 \chi_j^-}^L g_{H^- \chi_k^0 \chi_j^+}^R](D_0 + D_1 + D_2 + D_3) \\ & + m_{\chi_i^0} m_{\chi_k^0} g_{e \chi_i^0 \tilde{e}_L}^L g_{e \chi_k^0 \tilde{e}_L}^L g_{H^+ \chi_i^0 \chi_j^-}^L g_{H^- \chi_k^0 \chi_j^+}^L (D_1 + D_2 + D_3)](I_A + I_V) \end{aligned} \quad (D.3)$$

With

$$D_m \equiv D_m(m_{H^\pm}^2, m_e^2, m_e^2, m_{H^\pm}^2, t, s, m_{\chi_j^+}^2, m_{\chi_i^0}^2, m_{\tilde{e}_L}^2, m_{\chi_k^0}^2)_{m=0,\dots,3}$$

Where:

$$g_{H^+\chi_i^0\chi_j^-}^L = -\frac{\cos\beta}{s_W}(\frac{1}{\sqrt{2}}V_{j2}(Z_{i2} + Z_{i1}\frac{s_W}{c_W}) + Z_{i4}V_{j1})$$

$$g_{H^-\chi_i^0\chi_j^+}^R = -\frac{\sin\beta}{s_W}(-\frac{1}{\sqrt{2}}U_{j2}(Z_{i2} + Z_{i1}\frac{s_W}{c_W}) + Z_{i3}U_{j1})\epsilon_i$$

In the case of right selectron  $\tilde{e}_R$ :

$$M_{1.18R} = -\frac{\alpha^2}{2} \sum_{i=1}^4 \sum_{j=1}^2 \sum_{k=1}^4 [(g_{e\chi_i^0\tilde{e}_R}^R g_{e\chi_k^0\tilde{e}_R}^R g_{H^+\chi_i^0\chi_j^-}^L g_{H^-\chi_k^0\chi_j^+}^L)((m_{\chi_j^+}^2 + m_{\tilde{e}_R}^2 - t)D_0 +$$

$$C_0[m_{H^\pm}^2, m_{H^\pm}^2, s, m_{\chi_i^0}^2, m_{\chi_j^+}^2, m_{\chi_k^0}^2] + (m_{\chi_j^+}^2 - t)(D_1 + D_2 + D_3))$$

$$+ [m_{\chi_j^+} m_{\chi_k^0} g_{e\chi_i^0\tilde{e}_R}^R g_{e\chi_k^0\tilde{e}_R}^R g_{H^+\chi_i^0\chi_j^-}^L g_{H^-\chi_k^0\chi_j^+}^R$$

$$+ m_{\chi_j^+} m_{\chi_i^0} g_{e\chi_i^0\tilde{e}_R}^R g_{e\chi_k^0\tilde{e}_R}^R g_{H^+\chi_i^0\chi_j^-}^L g_{H^-\chi_k^0\chi_j^+}^L](D_0 + D_1 + D_2 + D_3)$$

$$+ m_{\chi_i^0} m_{\chi_k^0} g_{e\chi_i^0\tilde{e}_R}^R g_{e\chi_k^0\tilde{e}_R}^R g_{H^+\chi_i^0\chi_j^-}^R g_{H^-\chi_k^0\chi_j^+}^R (D_1 + D_2 + D_3)](I_V - I_A) \quad (D.4)$$

with

$$D_m \equiv D_m(m_{H^\pm}^2, m_e^2, m_e^2, m_{H^\pm}^2, t, s, m_{\chi_j^+}^2, m_{\chi_i^0}^2, m_{\tilde{e}_R}^2, m_{\chi_k^0}^2)_{m=0,\dots,3}$$

$$g_{e\chi_i^0\tilde{e}_R}^L = -\sqrt{2}(N_{i1}^{'*} - \frac{s_W}{c_W}N_{i2}^{'*}))$$

### Crossed box 1.18

For Majorana particles, we can have three propagators  $u\bar{u}$ ,  $uu$  and  $\bar{u}\bar{u}$  as a consequence of the clashing in the propagator of Majorana particle the box of figure 1.18 has a crossed one. The amplitude is given by:

$$\mathcal{M}_{cross1.18L} = \frac{\alpha^2}{2} \sum_{i=1}^4 \sum_{j=1}^2 \sum_{k=1}^4 [ g_{e\chi_i^0\tilde{e}_L}^L g_{e\chi_k^0\tilde{e}_L}^L g_{H^-\chi_i^0\chi_j^-}^L g_{H^+\chi_k^0\chi_j^+}^L ((m_{\chi_j^+}^2 + m_{\tilde{e}_L}^2 - u) D_0$$

$$+ C_0[m_{H^\pm}^2, m_{H^\pm}^2, s, m_{\chi_i^0}^2, m_{\chi_j^+}^2, m_{\chi_k^0}^2] + (m_{\chi_j^+}^2 - u) (D_1 + D_2 + D_3))$$

$$+ [m_{\chi_j^+} m_{\chi_i^0} g_{e\chi_i^0\tilde{e}_L}^L g_{e\chi_k^0\tilde{e}_L}^L g_{H^-\chi_i^0\chi_j^-}^R g_{H^+\chi_k^0\chi_j^+}^L$$

$$+ m_{\chi_j^+} m_{\chi_k^0} g_{e\chi_i^0\tilde{e}_L}^L g_{e\chi_k^0\tilde{e}_L}^L g_{H^-\chi_i^0\chi_j^-}^L g_{H^+\chi_k^0\chi_j^+}^R] (D_0 + D_1 + D_2 + D_3)$$

$$+ m_{\chi_i^0} m_{\chi_k^0} g_{e\chi_i^0\tilde{e}_L}^L g_{e\chi_k^0\tilde{e}_L}^L g_{H^-\chi_i^0\chi_j^-}^R g_{H^+\chi_k^0\chi_j^+}^R (D_1 + D_2 + D_3)](I_A + I_V) \quad (D.5)$$

with

$$D_m \equiv D_m(m_{H^\pm}^2, m_e^2, m_e^2, m_{H^\pm}^2, u, s, m_{\chi_j^+}^2, m_{\chi_k^0}^2, m_{\tilde{e}_L}^2, m_{\chi_i^0}^2)_{m=0,\dots,3}$$

In the case of right selectron  $\tilde{e}_R$ :

$$\begin{aligned}
\mathcal{M}_{cross1.18R} = & \frac{\alpha^2}{2} \sum_{i=1}^4 \sum_{j=1}^2 \sum_{k=1}^4 [ g_{e\chi_i^0\tilde{e}_R}^R g_{e\chi_k^0\tilde{e}_R}^R g_{H^-\chi_i^0\chi_j^-}^R g_{H^+\chi_k^0\chi_j^+}^R ((m_{\chi_j^+}^2 + m_{\tilde{e}_R}^2 - u) D_0 + \\
& C_0[m_{H^\pm}^2, m_{H^\pm}^2, s, m_{\chi_i^0}^2, m_{\chi_j^+}^2, m_{\chi_k^0}^2] + (m_{\chi_j^+}^2 - u) (D_1 + D_2 + D_3)) \\
& + [m_{\chi_j^+} m_{\chi_i^0} g_{e\chi_i^0\tilde{e}_R}^R g_{e\chi_k^0\tilde{e}_R}^R g_{H^-\chi_i^0\chi_j^-}^L g_{H^+\chi_k^0\chi_j^+}^R \\
& + m_{\chi_j^+} m_{\chi_k^0} g_{e\chi_i^0\tilde{e}_R}^R g_{e\chi_k^0\tilde{e}_R}^R g_{H^-\chi_i^0\chi_j^-}^R g_{H^+\chi_k^0\chi_j^+}^L] (D_0 + D_1 + D_2 + D_3) \\
& + m_{\chi_i^0} m_{\chi_k^0} g_{e\chi_i^0\tilde{e}_R}^R g_{e\chi_k^0\tilde{e}_R}^R g_{H^-\chi_i^0\chi_j^-}^L g_{H^+\chi_k^0\chi_j^+}^L (D_1 + D_2 + D_3)] (I_V - I_A) \quad (D.6)
\end{aligned}$$

With

$$D_m \equiv D_m(m_{H^\pm}^2, m_e^2, m_e^2, m_{H^\pm}^2, u, s, m_{\chi_j^+}^2, m_{\chi_k^0}^2, m_{\tilde{e}_R}^2, m_{\chi_i^0}^2)_{m=0,\dots,3}$$

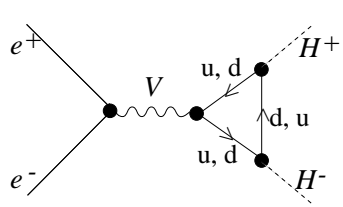
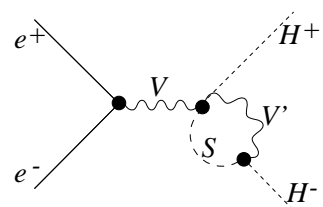
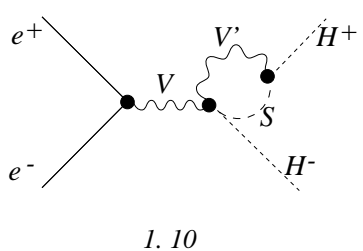
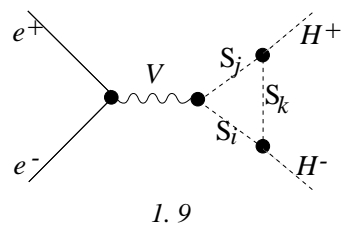
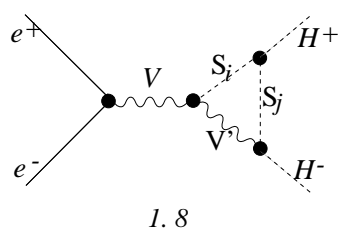
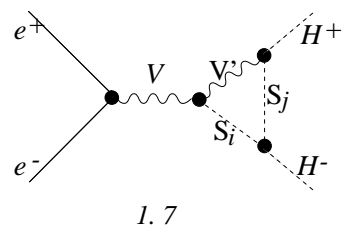
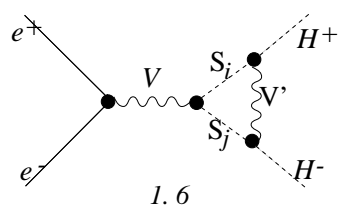
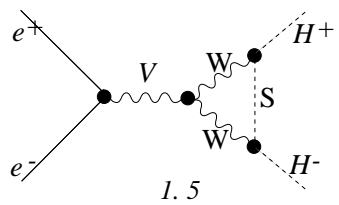
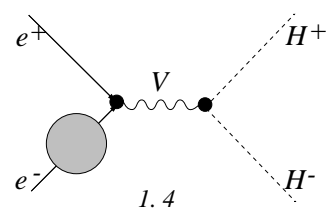
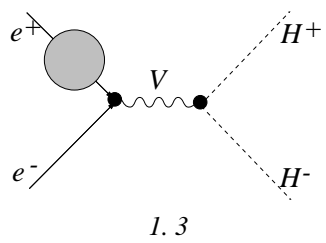
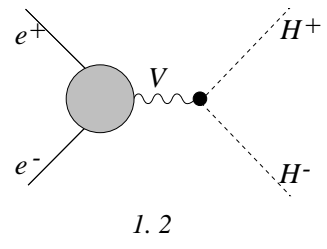
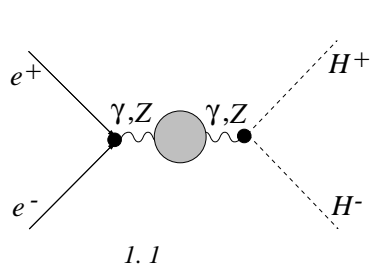
**box 1.17**

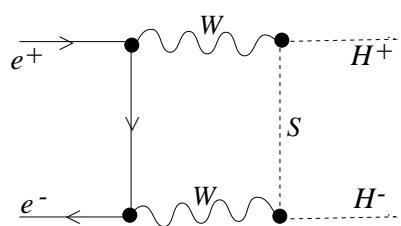
$$\begin{aligned}
\mathcal{M}_{1.17} = & \frac{\alpha^2}{2} \sum_{i=1}^2 \sum_{j=1}^4 \sum_{k=1}^2 [g_{e\chi_i^+\tilde{\nu}}^L g_{e\chi_k^+\tilde{\nu}}^L g_{H^+\chi_i^0\chi_j^-}^R g_{H^-\chi_k^0\chi_j^+}^R ((m_{\chi_j^0}^2 + m_{\tilde{\nu}}^2 - t) D_0 + \\
& C_0[m_{H^\pm}^2, m_{H^\pm}^2, s, m_{\chi_k^+}^2, m_{\chi_j^0}^2, m_{\chi_i^+}^2] + (m_{\chi_j^0}^2 - t) (D_1 + D_2 + D_3)) - \\
& [m_{\chi_j^0} m_{\chi_k^+} g_{e\chi_i^+\tilde{\nu}}^L g_{e\chi_k^+\tilde{\nu}}^L g_{H^+\chi_i^0\chi_j^-}^R g_{H^-\chi_k^0\chi_j^+}^L + \\
& m_{\chi_i^+} m_{\chi_j^0} g_{e\chi_i^+\tilde{\nu}}^L g_{e\chi_k^+\tilde{\nu}}^L g_{H^+\chi_i^0\chi_j^-}^L g_{H^-\chi_k^0\chi_j^+}^R] (D_0 + D_1 + D_2 + D_3) + \\
& + m_{\chi_i^+} m_{\chi_k^+} g_{e\chi_i^+\tilde{\nu}}^L g_{e\chi_k^+\tilde{\nu}}^L g_{H^+\chi_i^0\chi_j^-}^L g_{H^-\chi_k^0\chi_j^+}^L (D_1 + D_2 + D_3)] (I_A + I_V) \quad (D.7)
\end{aligned}$$

with

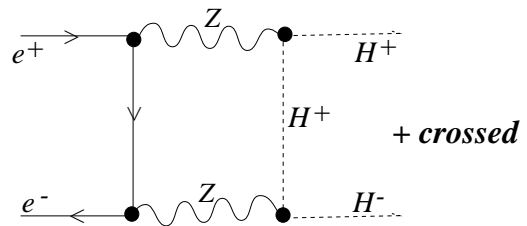
$$D_m \equiv D_m(m_{H^\pm}^2, m_e^2, m_e^2, m_{H^\pm}^2, t, s, m_{\chi_j^0}^2, m_{\chi_i^+}^2, m_{\tilde{\nu}}^2, m_{\chi_k^+}^2)_{m=0,\dots,3}$$

Finally we note that the amplitude corresponding to diagram 1.19 is negligibly small, being proportional to the electron mass.

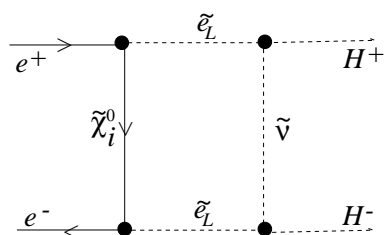




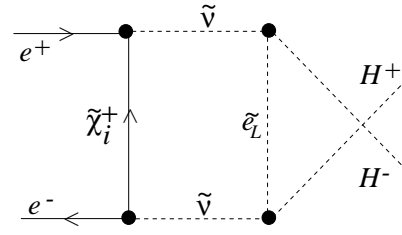
1. 13



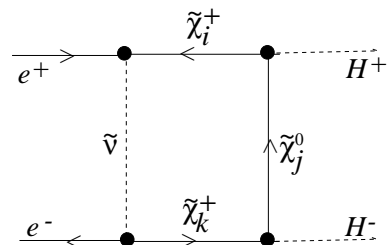
1. 14



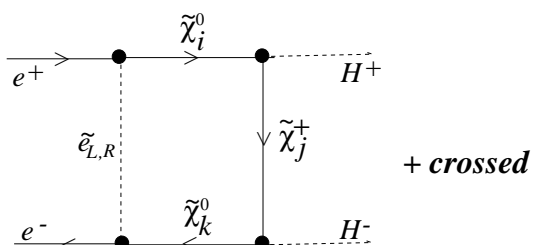
1. 15



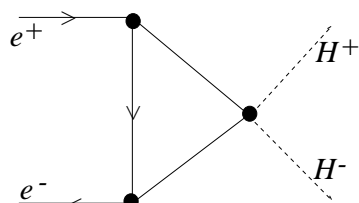
1. 16



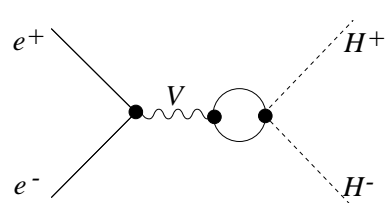
1. 17



1. 18

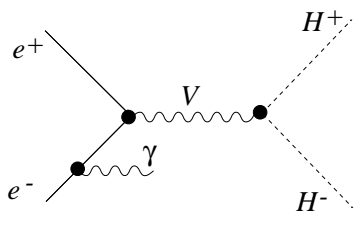


1. 19

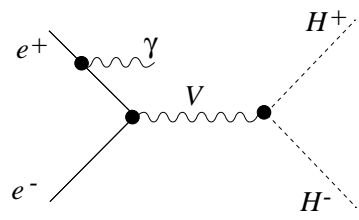


1. 20

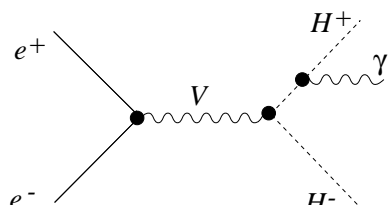
Fig 1 (cont.)



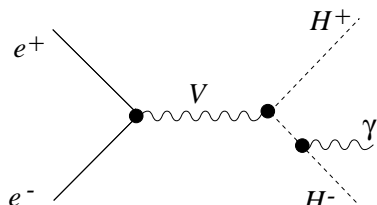
I. 21



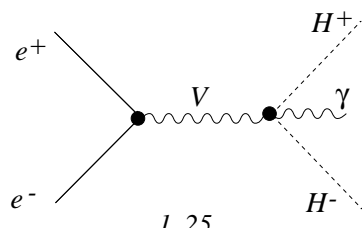
I. 22



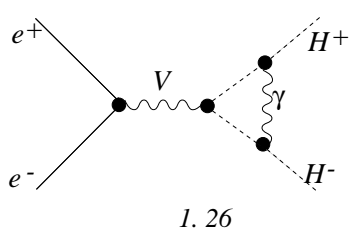
I. 23



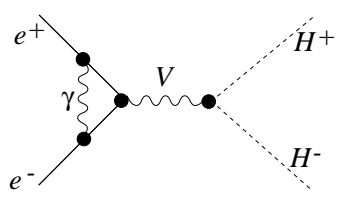
I. 24



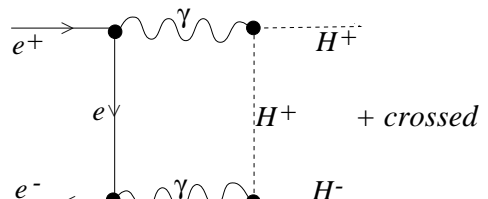
I. 25



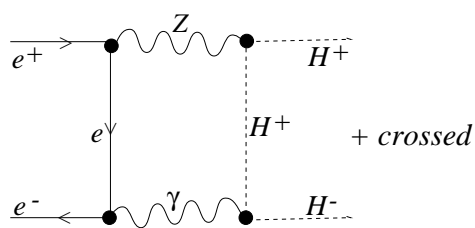
I. 26



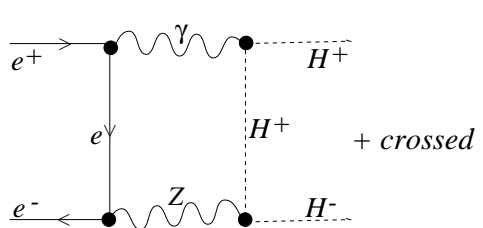
I. 27



I. 28



I. 29



I. 30

Fig 1 (cont.)

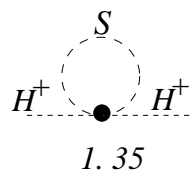
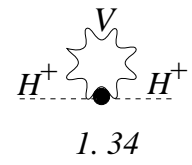
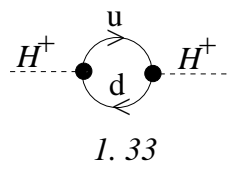
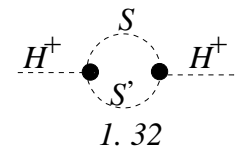
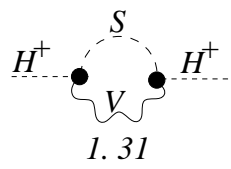


Fig 1 (cont.)

Fig 2.

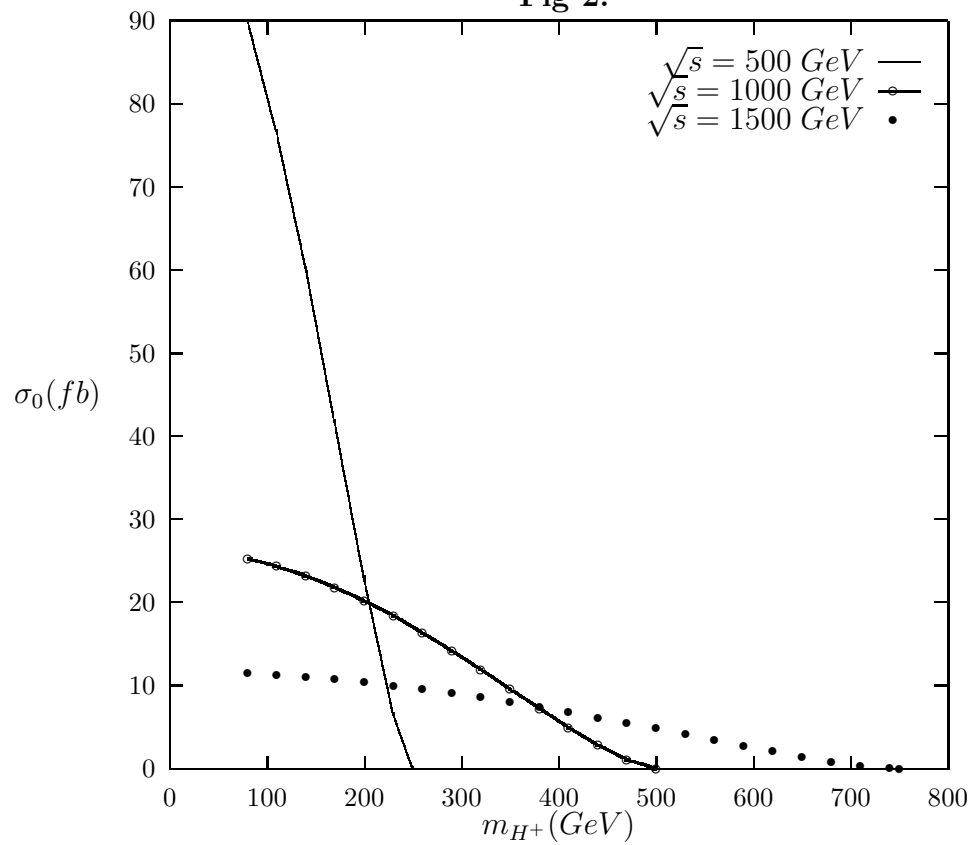


Fig 3. a

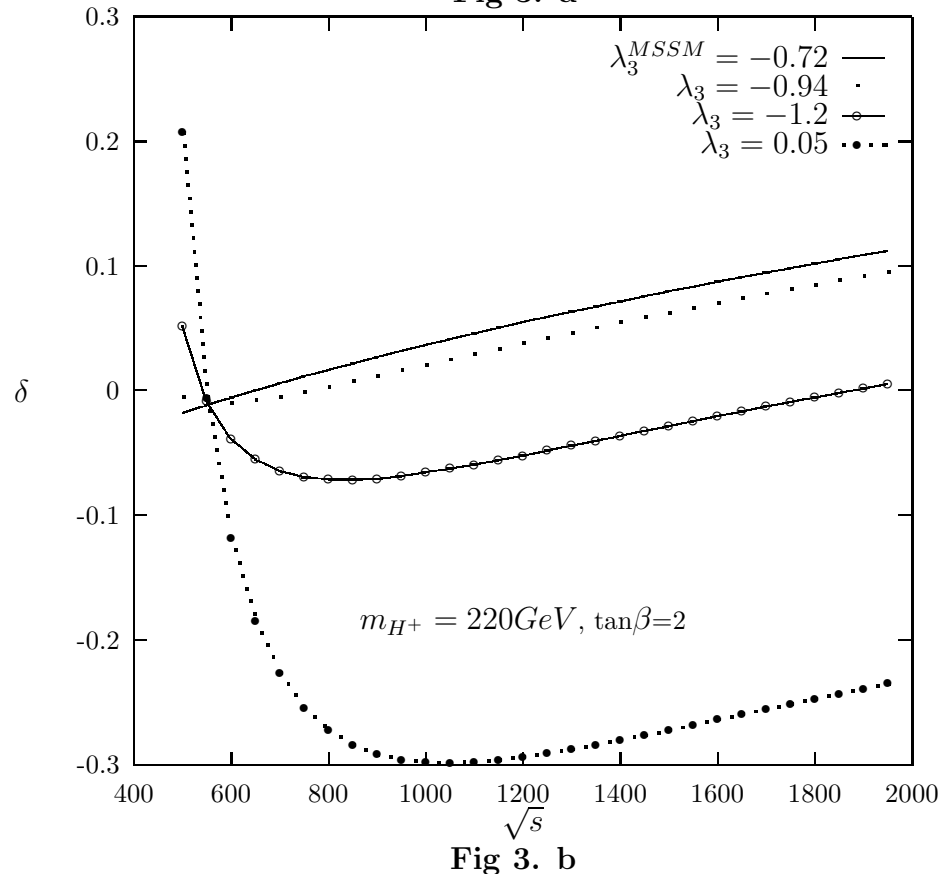


Fig 3. b

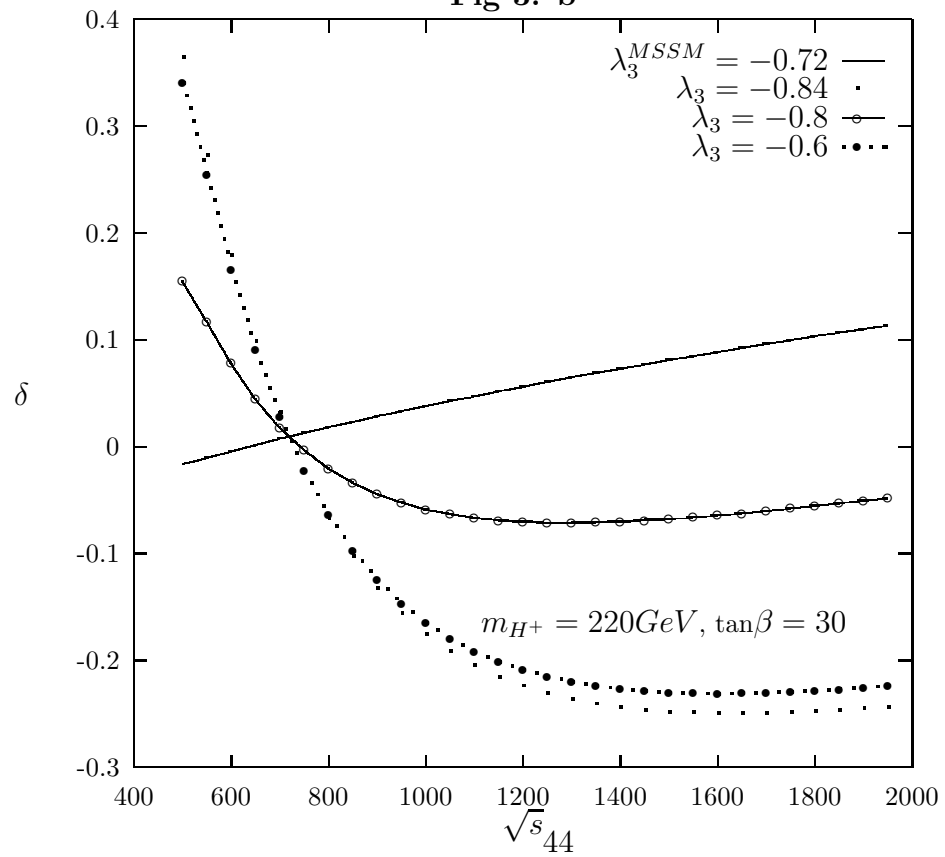


Fig 4. a

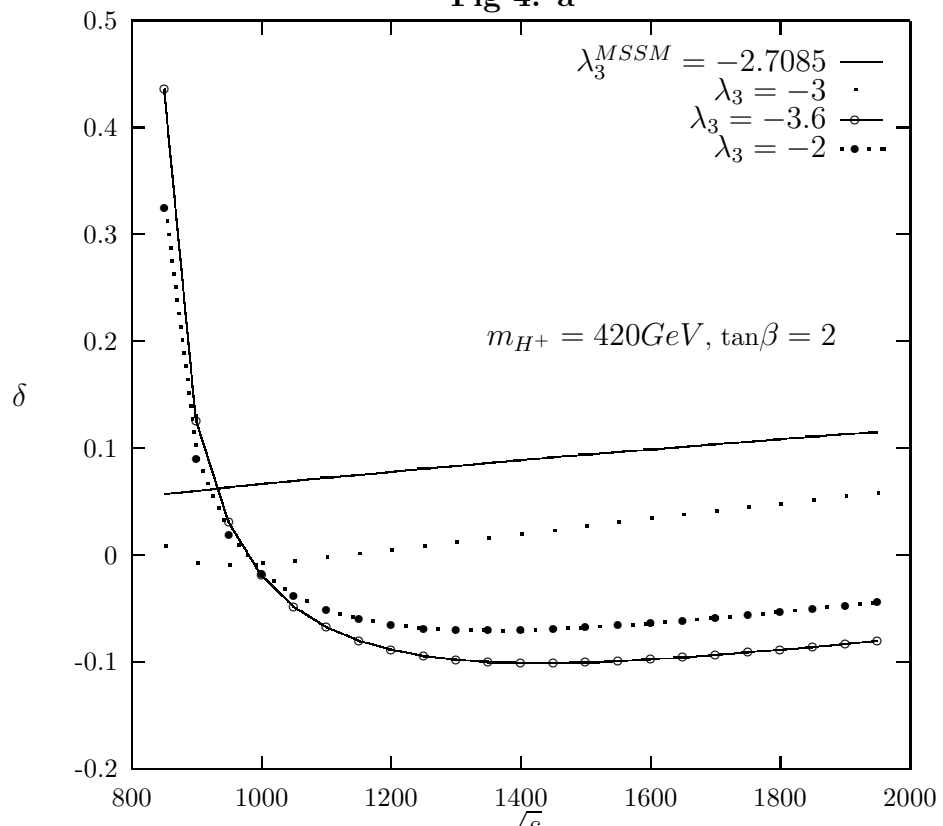
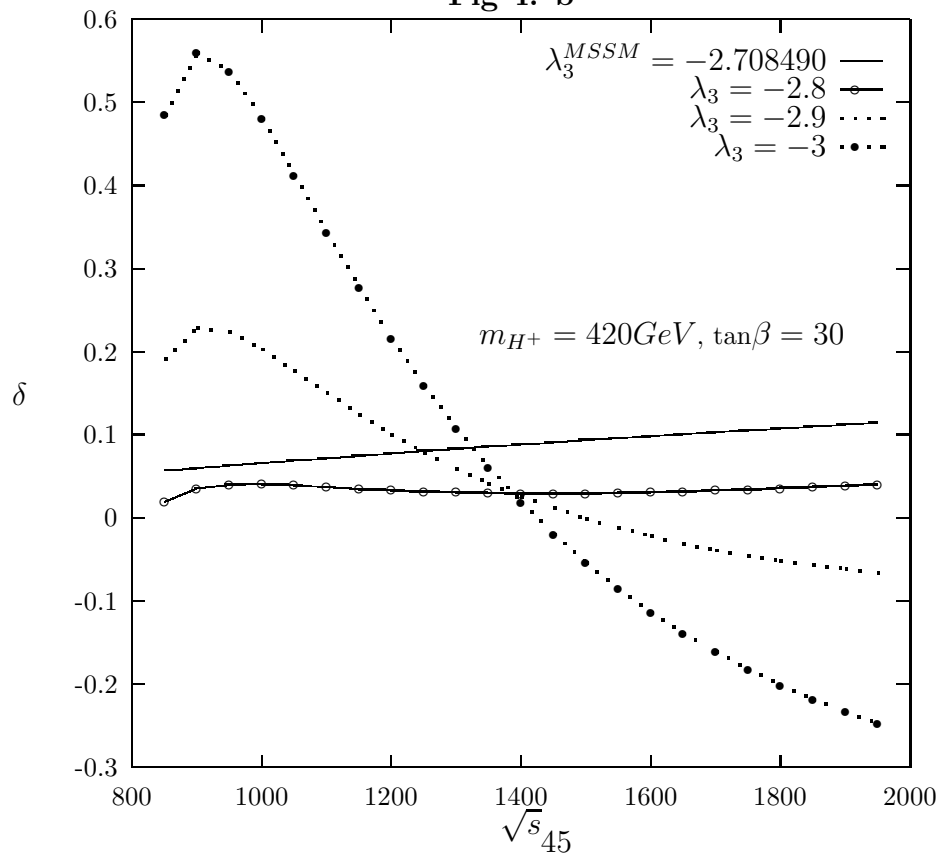
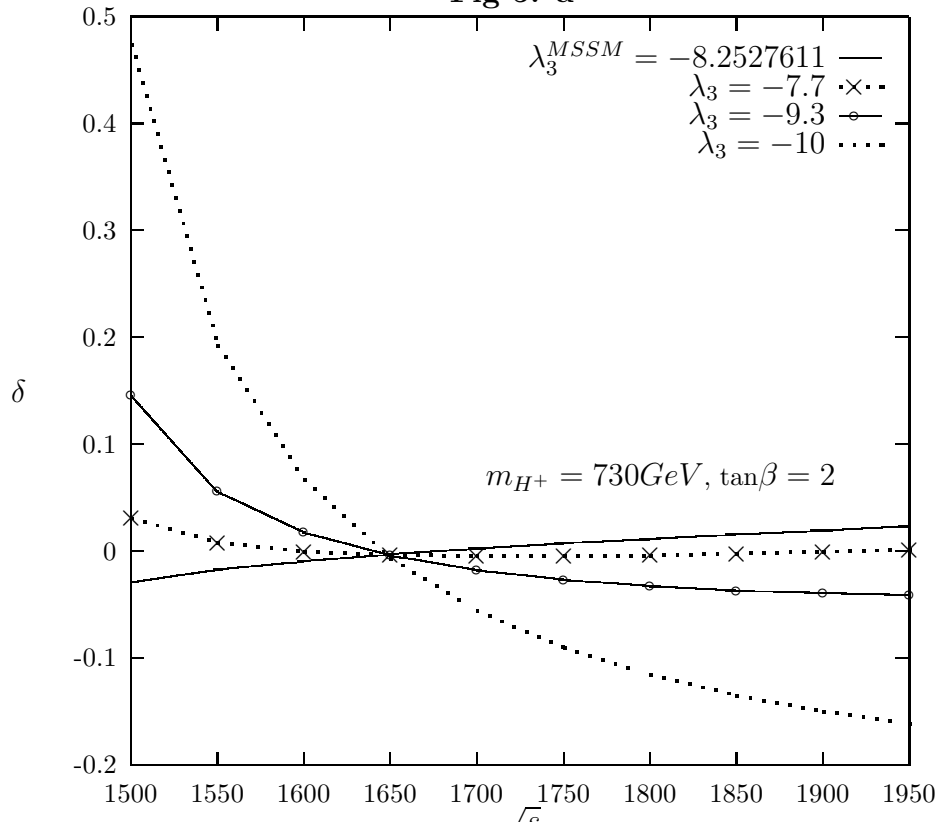


Fig 4. b



**Fig 5. a**



**Fig 5. b**

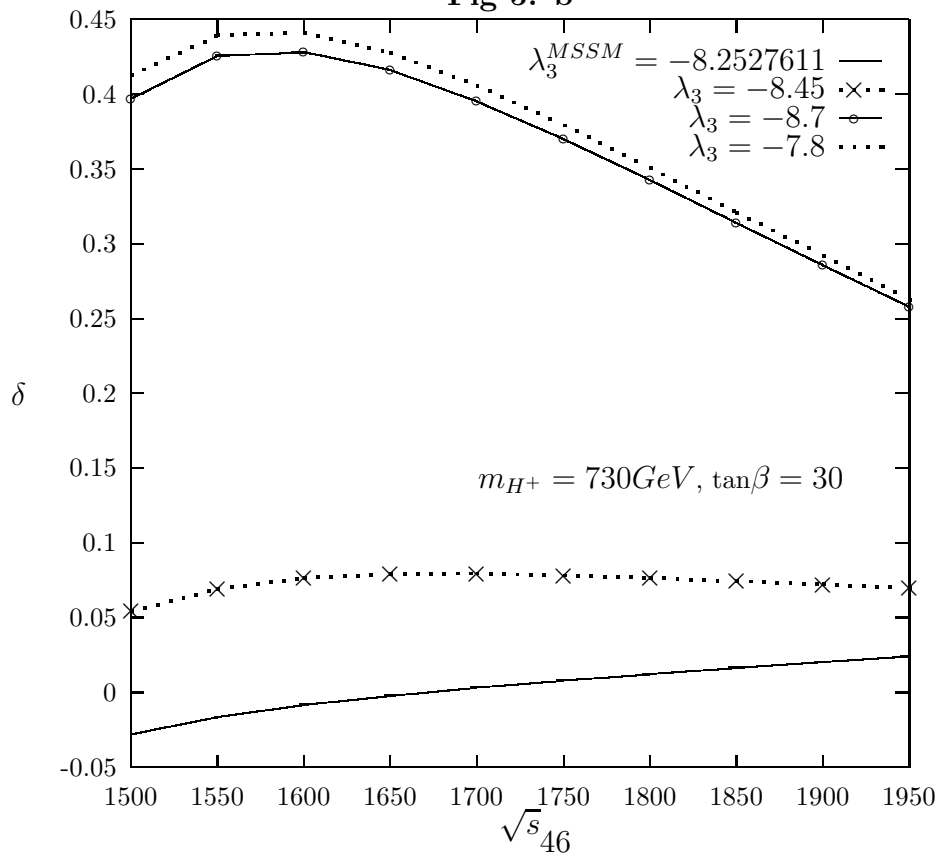


Fig 6. a

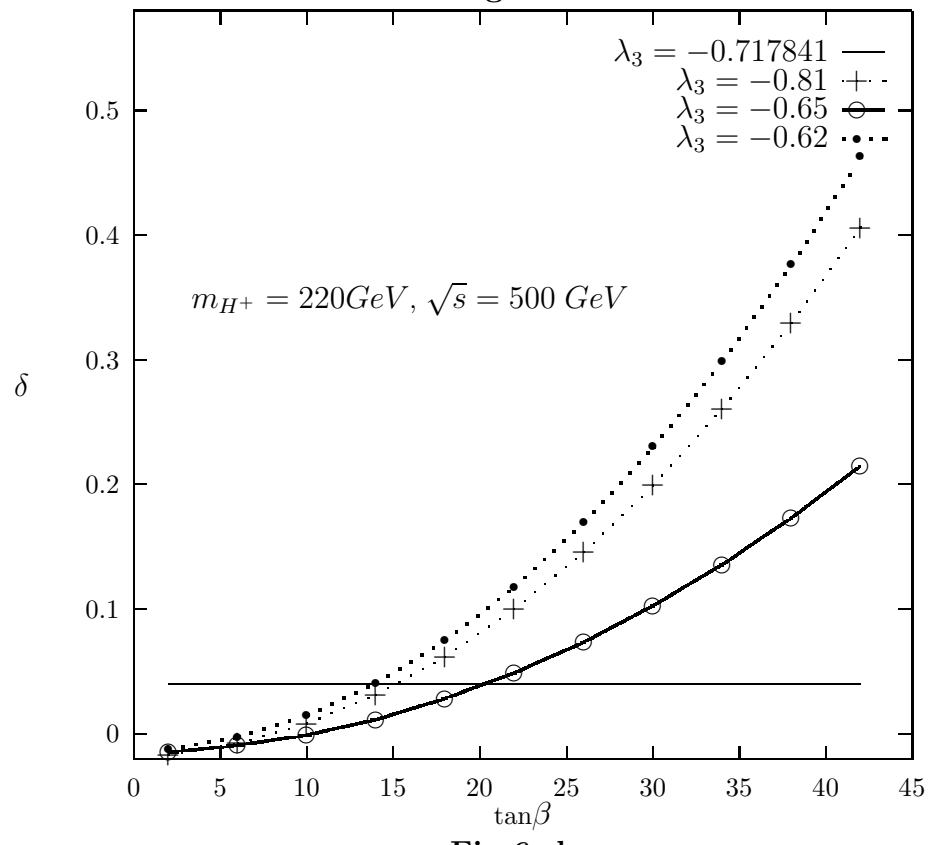
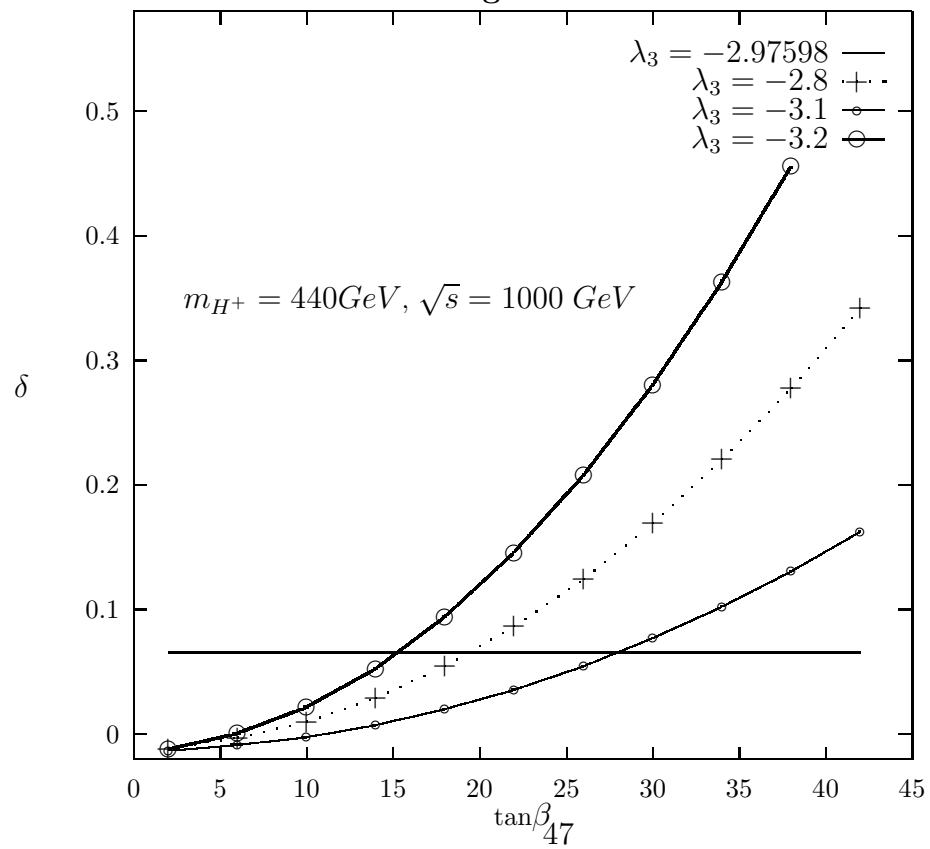
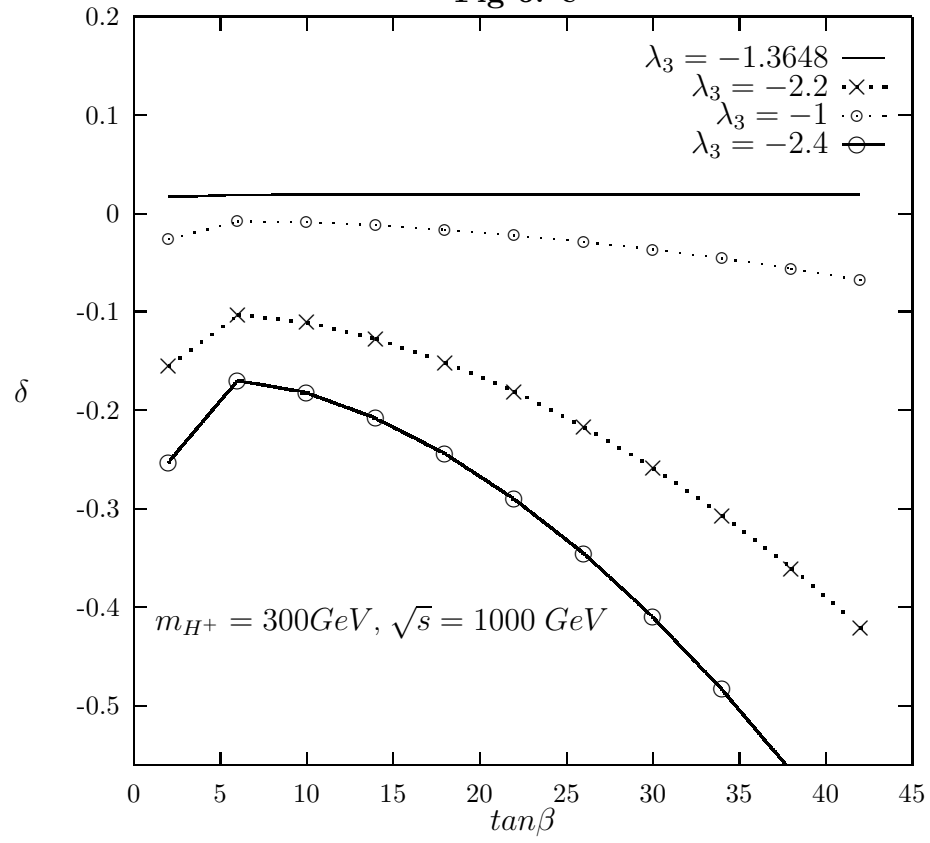


Fig 6. b



**Fig 6. c**



**Fig 7.**

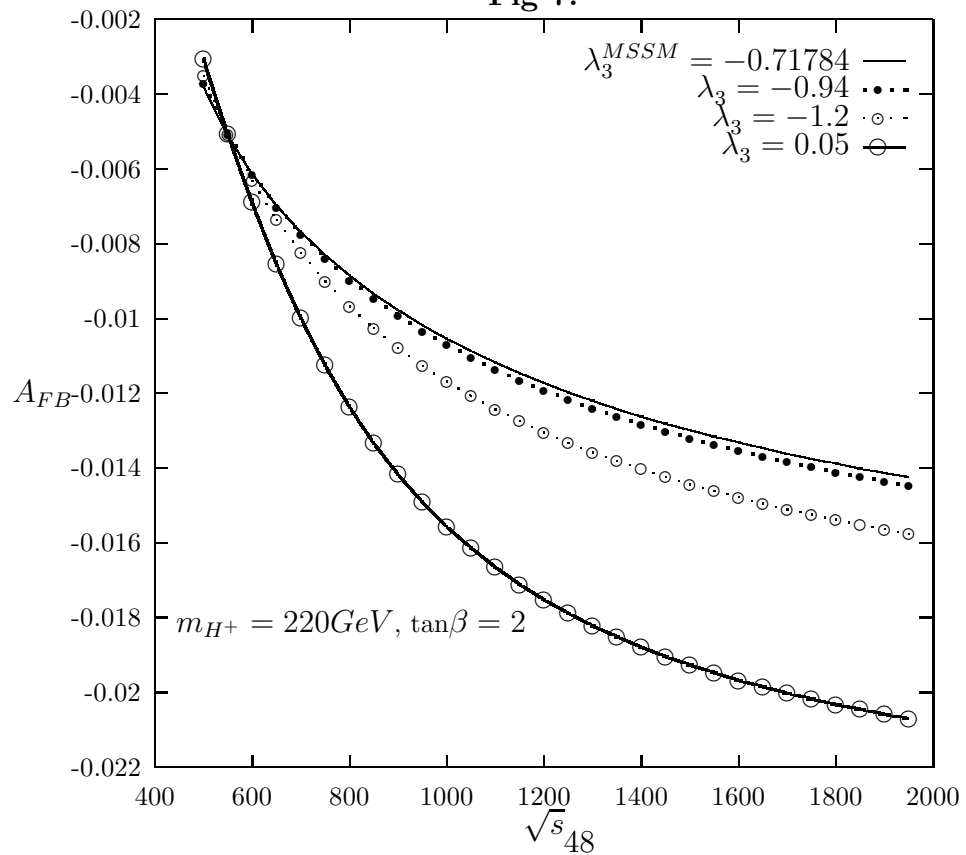


Fig 8. a

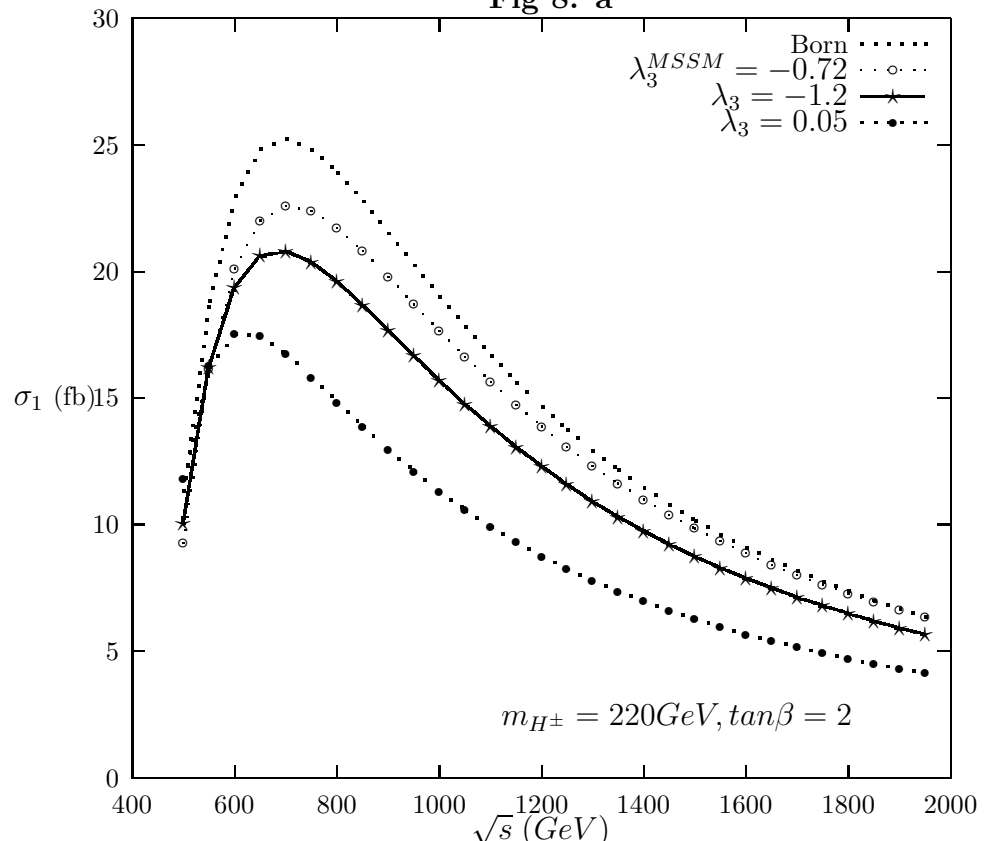


Fig 8. b

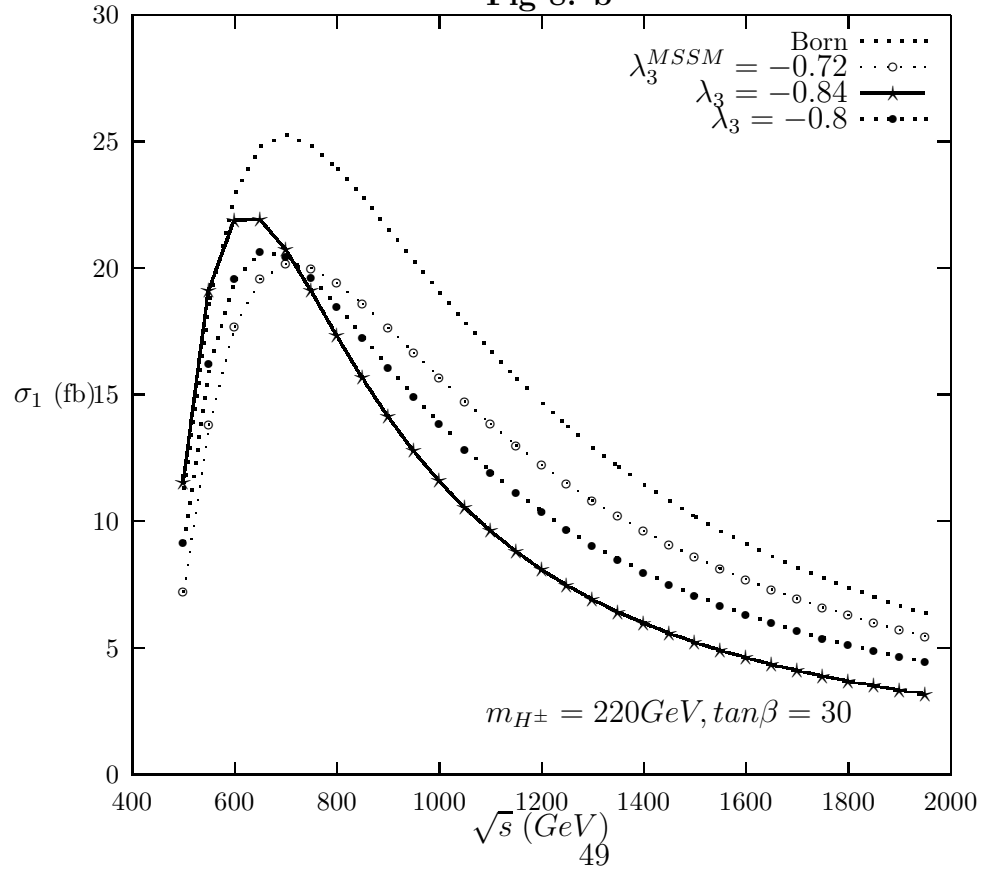


Fig 9. a

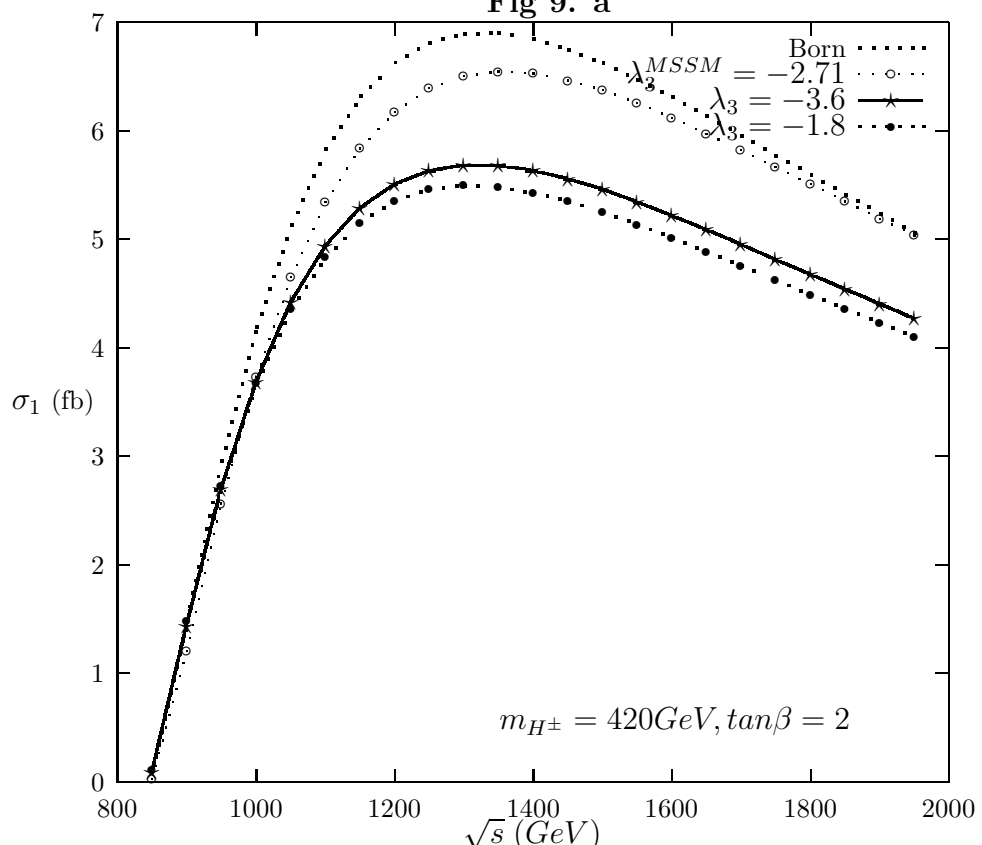


Fig 9. b

